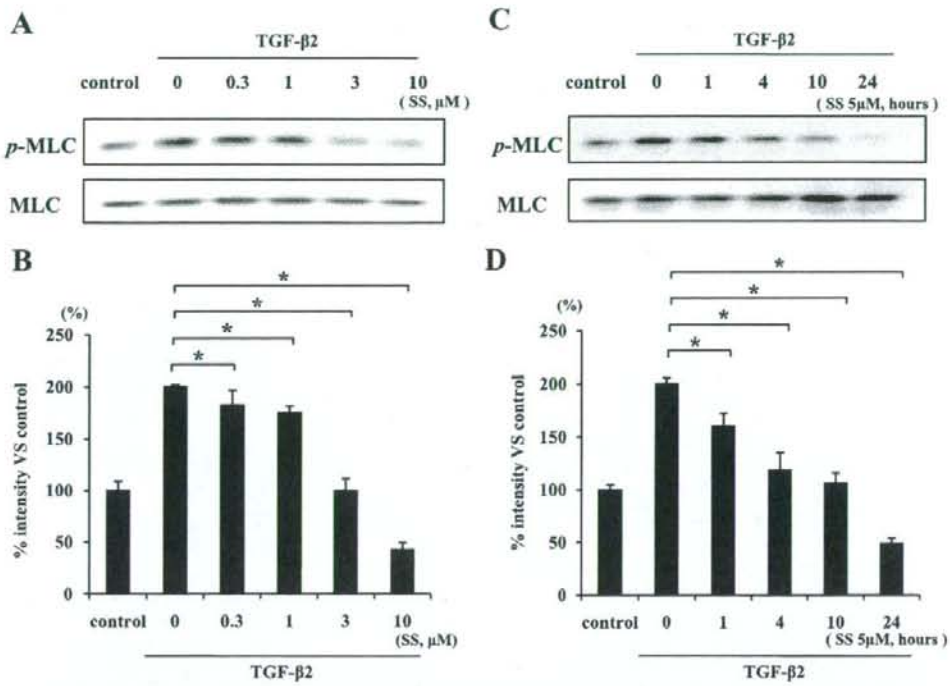


**FIG. 2. Inhibitory effect of simvastatin on TGF-β2–dependent MLC phosphorylation. Hyalocytes were starved in Dulbecco's modified Eagle's medium containing 3% calf serum for 24 h. *A*: Hyalocytes were pretreated for 30 min with or without the indicated concentrations of simvastatin (0.3, 1, 3, and 10 μmol/l) and subsequently treated with 3 ng/ml TGF-β2 for 24 h. Total cell lysates were subjected to Western blot analysis with an antibody against *p*-MLC. Lane loading differences were normalized by reblotting the membranes with an antibody against MLC. *C*: Hyalocytes were pretreated with or without 5 μmol/l simvastatin for the indicated time (1, 4, 10, and 24 h) and subsequently treated with 3 ng/ml TGF-β2 for 24 h. *p*-MLC and MLC were also examined in the same way as in Fig. 1*A*. *B* and *D*: Signal intensity ratios (*p*-MLC to MLC) were expressed as percentage of control intensity ratio. *$P < 0.05$ compared with TGF-β2 alone.**

Heights, IL) detection system. Lane loading differences were normalized by reblotting the membranes with an antibody against MLC (Santa Cruz) (1:1,000).

Plasma membrane proteins from the cells were isolated by Qproteome Plasma Membrane Protein kit (Qiagen, Hilden, Germany) and were subjected to Western blot analysis with an antibody against Rho (1:1,000; Upstate, Charlottesville, VA).

**Counting viable cells in collagen gels.** After 5 days of treatment, the collagen gels were dissolved by collagenase, and the cell suspension was collected. The viable cell number was counted with hemocytometer after trypan blue staining.

**In vivo model of PVR.** All experimental procedures using animals adhered to the Association for Research in Vision and Ophthalmology Resolution on the Use of Animals in Ophthalmic and Vision Research. We caused experimental PVR in rabbit eyes as previously described (34). Homologous conjunctival fibroblasts were prepared by harvesting the conjunctival tissue. Twenty eyes from 20 Dutch rabbits weighing 2–2.5 kg were assigned into three groups, and fibroblasts (100,000 cells) were injected into the right eye in each rabbit. Eyes in the first group (six eyes) were administered an intravitreal injection of 0.1 ml vehicle (balanced salt solution). Eyes in the second group (seven eyes) were administered an intravitreal injection of 0.1 ml vehicle containing simvastatin (5 μmol/l final intravitreal concentration). Eyes in the last group (seven eyes) were administered an intravitreal injection of 0.1 ml vehicle containing simvastatin (15 μmol/l final intravitreal concentration). The clinical observations were performed carefully as long as 28 days after surgery and categorized according with the PVR classification of Fastenberg et al. (35).

**Electroretinography.** Nine eyes from 10 Dutch rabbits weighing 2–2.5 kg were assigned into three groups. Eyes in the first group (three eyes) were administered an intravitreal injection of 0.1 ml vehicle. Eyes in the second group (three eyes) were administered an intravitreal injection of 0.1 ml vehicle containing simvastatin (5 μmol/l final intravitreal concentration). Eyes in the third group (three eyes) were administered an intravitreal injection of 0.1 ml vehicle containing simvastatin (15 μmol/l final intravitreal concentration). Electroretinogram was performed on day 28 as previously described (36).

**Light microscopy.** The eyes were enucleated and fixed in 4% paraformaldehyde on day 28. Whole eyes were cut approximately along the vertical meridian. Paraffin-embedded sections were stained with hematoxylin-eosin, and each section was examined using light microscopy.

**TdT-dUTP terminal nick-end labeling assay.** Apoptotic and potentially necrotic cell death was detected by TdT-dUTP terminal nick-end labeling (TUNEL). The eyes were fixed in 4% paraformaldehyde and embedded in paraffin. TUNEL staining was performed with the TdT Fluorescein in situ apoptosis detection kit (R&D Systems), according to the manufacturer's protocols. The sections were costained with propidium iodide (Molecular Probes, Eugene, OR) to observe the cell nuclei by fluorescence microscopy (KEYENCE, BIORAVO, and BZ-9000). As a TUNEL-positive control, we used the retina of rabbit PVR model on day 7 after the onset.

**Transmission electron microscopy.** The eyes were fixed in 1% glutaraldehyde and 1% paraformaldehyde in PBS. The specimens were postfixed in veronal acetate buffer osmium tetroxide (2%), dehydrated in ethanol and water, and embedded in Epon. Ultrathin sections were cut from blocks and mounted on copper grids. The specimens were observed with an electron microscope (H7650; Hitachi, Tokyo).

**Statistical analysis.** Statistical differences were assessed using nonparametric test (Kruskal-Wallis variance analysis) for the data of TGF-β2 concentrations and ANOVA for the other groups. $P$ values $<0.05$ were considered significant. To adjust for inflated α-error due to multiple comparisons, the corrected significant $P$ value was defined using the Bonferroni correction.

## RESULTS

**TGF-β2 in the vitreous and its impact on membrane contraction.** The median TGF-β2 protein concentrations, 2.35 ng/ml (range 0.72–5.26) in macular hole ($n = 27$), 4.74 ng/ml (1.60–13.0) in PDR ($n = 53$), and 4.48 ng/ml (2.52–21.6) in PVR ($n = 22$) patients, were significantly higher in PDR or PVR patients than in patients with macular hole ($P < 0.01$) (Fig. 1*A*). The median TGF-β2 protein concen-

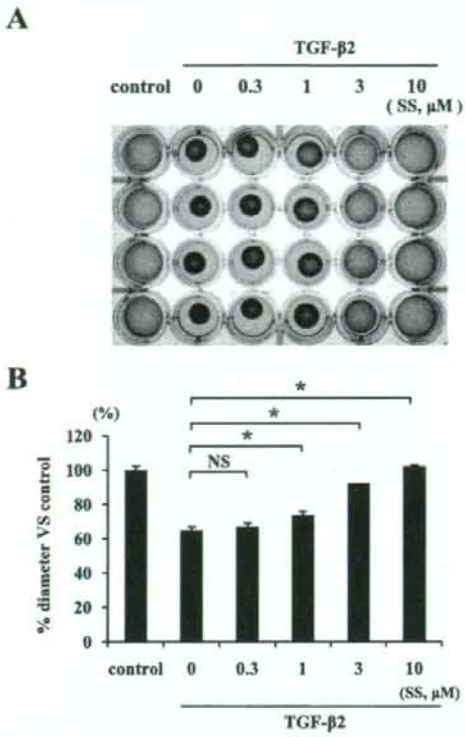


FIG. 3. The effect of simvastatin on TGF-β2–induced contraction of hyalocyte-containing collagen gels. Hyalocytes were embedded in type I collagen gels ($n$ = 4). *A*: After starvation and pretreatment with indicated concentrations of simvastatin for 24 h, the collagen gels were stimulated with 3 ng/ml TGF-β2. Five days after the stimulation, the gels were photographed. *B*: The diameter of the collagen gels was measured and expressed as a percentage of the average diameter of control group. *$P$ < 0.05; NS, not significant compared with TGF-β2 alone.

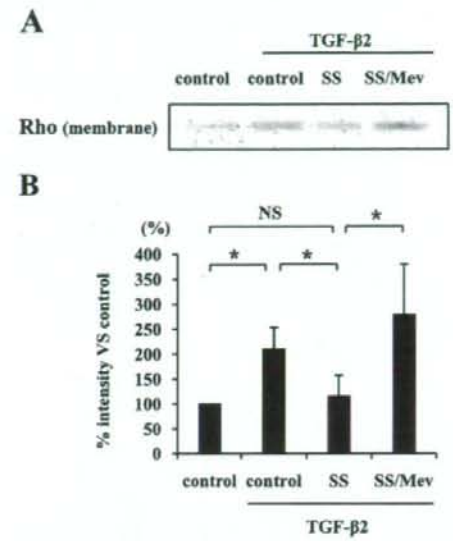


FIG. 4. Inhibitory effect of simvastatin on the Rho translocation to the plasma membrane. *A*: Hyalocytes were pretreated with 5 μmol/l simvastatin with or without mevalonate (Mev) and then treated with 3 ng/ml TGF-β2 for 24 h. Plasma membrane proteins were isolated and subjected to Western blot analysis with an antibody against Rho. *B*: Signal intensities were expressed as percentage of control intensity. *$P$ < 0.05.

tration in the vitreous samples from patients with PDR or PVR showed no significant difference ($P$ = 0.6).

Vitreous samples from patients with PVD and those containing nonspecific IgG induced significant contraction of hyalocyte-containing collagen gels (63 and 67% vs. control, respectively). In comparison, the vitreous-induced contraction was virtually suppressed by specific anti–TGF-β2 antibody ($P$ < 0.05) (97% vs. control) (Fig. 1*B* and *C*), suggesting a key role for TGF-β2 in the vitreous-induced collagen gel contraction.

**Role of simvastatin in TGF-β2–dependent MLC phosphorylation.** TGF-β2 enhanced MLC phosphorylation to about two times that seen with control (Fig. 2*A* and *B*). TGF-β2–dependent MLC phosphorylation showed a significant reduction at 0.3 μmol/l simvastatin or higher concentrations (up to 10 μmol/l simvastatin) compared with TGF-β2 alone ($P$ < 0.05). The level of MLC phosphorylation at 10 μmol/l simvastatin concentration was lower than in untreated control, suggesting that simvastatin at higher concentrations may block the constitutive level of MLC phosphorylation. Because 3 μmol/l simvastatin was sufficient to reverse the effect of TGF-β2 on MLC phosphorylation, we chose the slightly higher concentration of 5 μmol/l to study the time-dependent effect of simvastatin on TGF-β2–dependent MLC phosphorylation. Treatment of the hyalocytes with 5 μmol/l simvastatin for 1 h or longer (up to 24 h) significantly suppressed the MLC phosphorylation compared with TGF-β2 alone, and treatment with 5 μmol/l simvastatin for 24 h sufficiently suppressed the MLC phosphorylation below that of untreated control (Fig. 2*C* and *D*).

**TGF-β2–dependent collagen gel contraction and its inhibition by simvastatin.** The control gels showed no apparent contraction up to 5 days, whereas TGF-β2 caused substantial collagen gel contraction in a time-dependent manner in the first 5 days (57.6% vs. control). TGF-β2–dependent collagen gel contraction was significantly reduced by simvastatin starting at a concentration of 1 μmol/l, and the reduction was greater at 3 and 10 μmol/l (92 and 100% vs. control, respectively) (Fig. 3).

**TGF-β2–dependent Rho translocation to the plasma membrane and its inhibition by simvastatin.** TGF-β2 significantly enhanced the Rho translocation to the plasma membrane ($P$ < 0.05), whereas simvastatin suppressed the translocation (Fig. 4*A* and *B*). However, the effect of simvastatin was reversed in the presence of 400 μmol/l mevalonate, a component of the mevalonate pathway. These findings suggest that simvastatin inhibits Rho/Rho kinase pathway by preventing Rho from translocating to the plasma membrane via inhibition of the mevalonate pathway.

**Comparison of the effects of various statins on TGF-β2–dependent MLC phosphorylation and collagen gel contraction.** Simvastatin and fluvastatin significantly suppressed TGF-β2–dependent MLC phosphorylation by hyalocytes, whereas pravastatin did not show an effect (Fig. 5*A* and *B*). In addition, simvastatin significantly suppressed MLC phosphorylation compared with fluvastatin ($P$ < 0.05). Next, we compared the inhibitory effect of statins on the contraction of hyalocyte-containing collagen gels. Simvastatin and fluvastatin significantly suppressed TGF-β2–dependent contraction of collagen gel, whereas

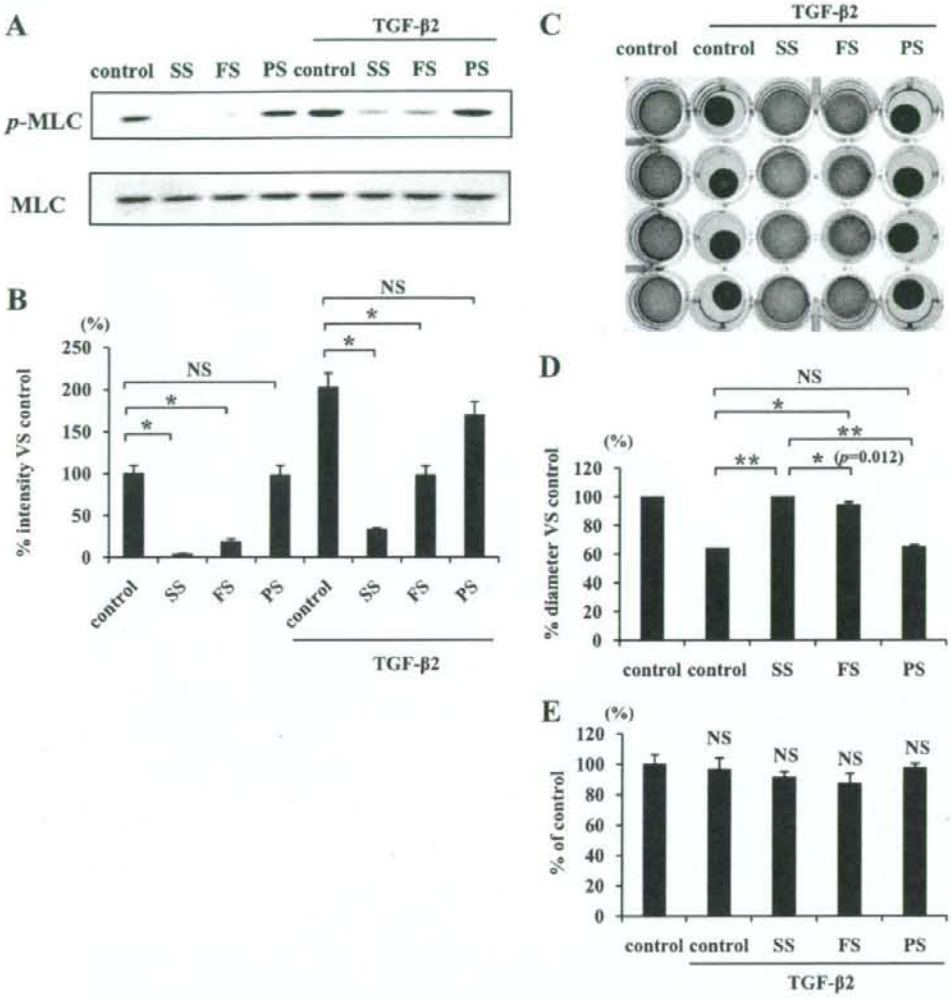


**FIG. 5. Comparison of inhibitory effects of simvastatin, fluvastatin, and pravastatin on TGF-β2–dependent MLC phosphorylation and collagen gel contraction. *A*: Starved hyalocytes were pretreated with vehicle, 5 μmol/l simvastatin, fluvastatin, or pravastatin for 30 min and subsequently treated with or without 3 ng/ml TGF-β2 for 24 h. Total cell lysates were subjected to Western blot analysis with an antibody against *p*-MLC. Lane loading differences were normalized by reblotting the membranes with an antibody against MLC. *B*: Signal intensity ratios (*p*-MLC to MLC) were expressed as percentage of intensity ratio of vehicle alone. *$P < 0.05$. *C*: Hyalocytes were embedded in type I collagen gels ($n = 4$). After starvation and pretreatment with vehicle, 5 μmol/l simvastatin, fluvastatin, or pravastatin for 24 h, the collagen gels were stimulated with 3 ng/ml TGF-β2. Five days after the stimulation, the gels were photographed. *D*: The diameter of the collagen gels was measured and expressed as percentage of the average diameter of control group. **$P < 0.01$, *$P < 0.05$; NS, not significant. *E*: The viable cell number in the collagen gels was counted to exclude the effect of cell growth or cytotoxicity on the collagen gel contraction or its inhibition. Five days after the treatment, the collagen gels were dissolved, and the cell suspension was collected. The viable cell number was counted with hemocytometer after trypan blue staining ($n = 4$; NS, not significant compared with control).**

pravastatin did not show an effect (Fig. 5*C* and *D*). In addition, the inhibitory effect of simvastatin (100% vs. control) was significantly higher than that by fluvastatin (94% vs. control) ($P < 0.05$). To test whether cytokine and/or statin treatment affected the growth and/or viability of the cells in our experiments, we treated the collagen gels with collagenase and counted the number of viable cells. Both TGF-β2 and statins showed no significant effects on cell number in the three-dimensional collagen gels (Fig. 5*E*).

**Impact of simvastatin on MLC phosphorylation and collagen gel contraction induced by vitreous samples from patients with PVD.** Vitreous samples from patients with PVD caused a significantly larger enhancement of MLC phosphorylation than those from patients with non-PVD (Fig. 6*A* and *B*). Simvastatin (5 μmol/l) strongly attenuated the vitreous-induced MLC phosphorylation. Expression of GAPDH did not change after the treatment with simvastatin or stimulation with vitreous samples. However, total MLC increased in cells stimulated with the vitreous samples compared with cells without vitreous treatment, and the increase was larger in cells stimulated with vitreous samples from patients with PVD than those from patients without PVD. These increases in an amount of total MLC were suppressed by 5 μmol/l simvastatin.

The contraction of hyalocyte-containing collagen gels stimulated with the vitreous samples from patients with PVD was significantly larger compared with the contrac-

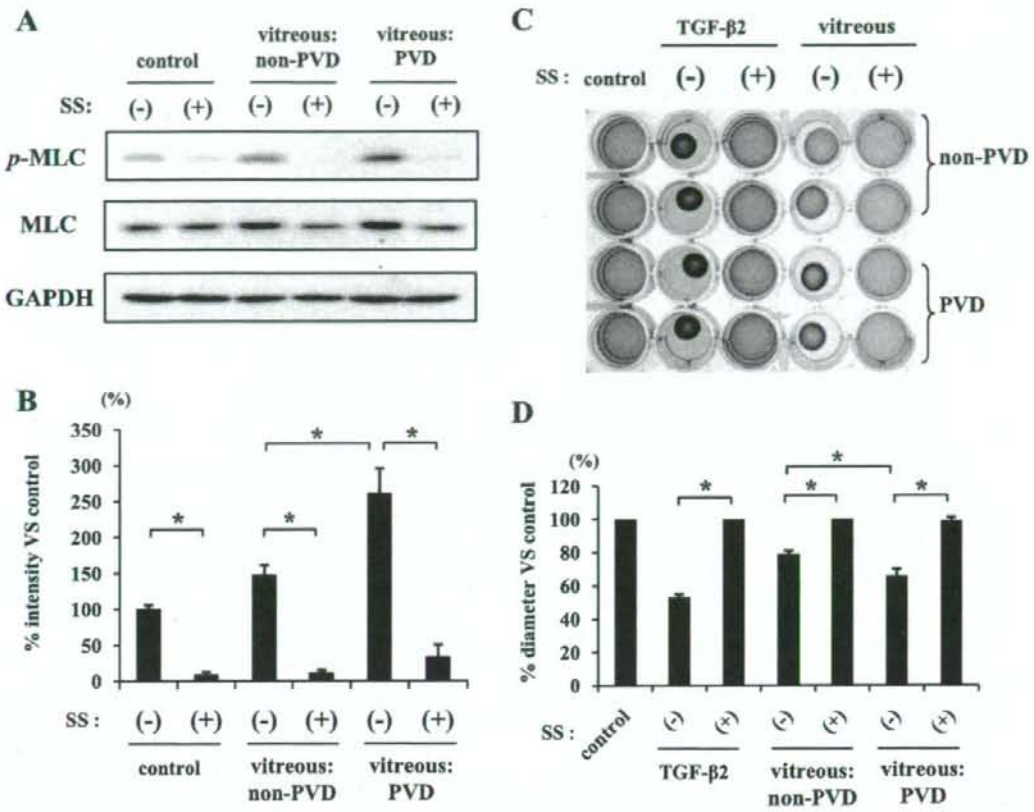


**FIG. 6. Inhibitory effects of simvastatin on vitreous-induced MLC phosphorylation and contraction of hyalocyte-containing collagen gels. *A*: Starved hyalocytes were pretreated with 5 μmol/l simvastatin for 30 min and subsequently treated with or without 400 μl vitreous samples of non-PVD (macular hole) or PVD (PDR and PVR) for 24 h. Total cell lysates were subjected to Western blot analysis with an antibody against *p*-MLC. Lane loading differences were normalized by reblotting the membranes with an antibody against MLC and GAPDH. *B*: Signal intensity ratios (*p*-MLC to GAPDH) were expressed as percentage of control intensity ratio. *C*: Hyalocytes were embedded in type I collagen gels ($n = 4$). After starvation and pretreatment with 5 μmol/l simvastatin for 24 h, the collagen gels were stimulated with 400 μl vitreous samples of non-PVD or PVD. Five days after the stimulation, the gels were photographed. *D*: The diameter of the collagen gels was measured and expressed as percentage of the average diameter of the control group. *$P < 0.05$.**

tion of the gels stimulated with vitreous samples from patients without PVD ($P < 0.05$) (Fig. 6*C* and *D*). We further examined the inhibitory effect of simvastatin on vitreous-dependent contraction of collagen gels and found that 5 μmol/l simvastatin suppressed the collagen gel contraction induced by vitreous samples even from patients with PVD.

**Simvastatin inhibition of PVR development in vivo.** The control eyes of rabbits injected with vehicle developed PVR and were accompanied by proliferative membrane formation and cicatricial contraction, resulting in tractional retinal detachment (Fig. 7*A*). In comparison, 5 and 15 μmol/l simvastatin (final intravitreal concentrations) significantly prevented PVR development (Fig. 7*C*). Simvastatin inhibited the contraction of the proliferative membrane, and the membranes in eyes treated with simvastatin were much thinner than those in vehicle-treated eyes (Fig. 7*B*). After simvastatin injections were stopped at day 7, the eyes treated with 5 μmol/l simvastatin developed a mild but significant PVR, whereas no significant PVR development was observed in the eyes treated with 15 μmol/l simvastatin.

**Absence of apparent adverse effects of simvastatin in the retina.** To evaluate the retinal function after intravitreal application of simvastatin, we performed electroretinography. The mean amplitude and latency of the 2Hz b wave in the eyes treated with 5 or 15 μmol/l simvastatin were 203.4 μV and 28.1 ms and 201.7 μV and 28.4 ms, respectively, and were not significantly different from those without any treatment or those of the vehicle-treated eyes (204.8 μV and 28.1 ms), suggesting that at these concentrations, simvastatin may not impede retinal function (Fig. 8*A*).

The histological structure of the retina in the eyes injected with simvastatin appeared normal when observed on day 28 (Fig. 8*B*, C).

In the retina of an experimental PVR used as a positive-control, apoptotic cells, which present TUNEL-positive staining (green), were detected in the inner nuclear layer and the outer nuclear layer (Fig. 8*D*). The eyes injected with simvastatin had no apparent TUNEL-positive staining in the retina when observed on day 28 (Fig. 8*E*).

The eyes injected with simvastatin had no apparent ultrastructual changes in internal limiting membrane,

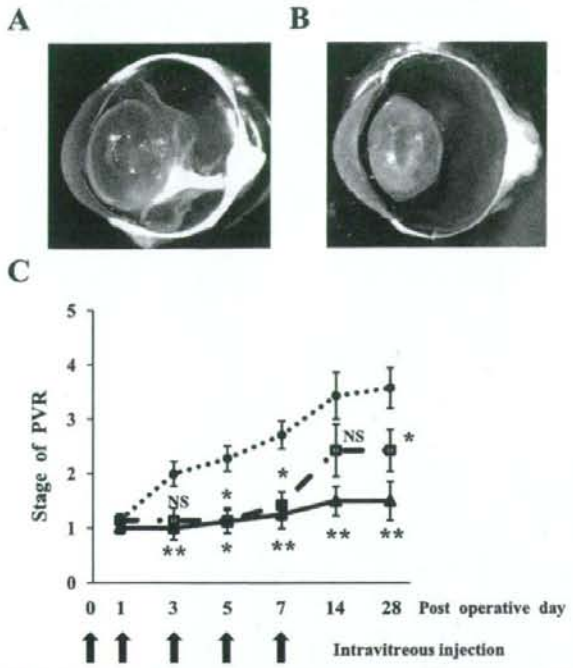


**FIG. 7. Inhibitory effects of simvastatin on experimental PVR in rabbit eyes. Rabbits underwent vitrectomy and intravitreal injection of fibroblasts with and without simvastatin on day 0. The eyes were injected with same contents of simvastatin on days 1, 3, 5, and 7 and examined using indirect ophthalmoscope as long as 28 days after the surgery. *A*: A representative vehicle-injected eye with PVR in stage 5, 28 days after the surgery. Proliferative membranes were observed in the vitreous cavity, causing a traction to the retina and retinal detachment. *B*: A representative simvastatin-injected eye (15 μmol/l) with PVR in stage 1. A thin proliferative membrane was observed, however, there was no evidence of tractional retinal detachment. *C*: Clinical observations were categorized according to the PVR classification of Fastenberg et al. (35). Stage 1, intravitreal membrane; stage 2, focal traction, localized vascular changes, hyperemia, engorgement, dilation, and blood vessel elevation; stage 3, localized detachment of medullary ray; stage 4, extensive retinal detachment, total medullary ray detachment, and peripapillary retinal detachment; and stage 5, total retinal detachment. ●, vehicle; □, 5 μmol/l simvastatin; ▲, 15 μmol/l simvastatin. **$P$ < 0.01, *$P$ < 0.05; NS, not significant compared with vehicle.**

nerve fiber layer, and ganglion cell layer (Fig. 8*G*) compared with the untreated control eyes (Fig. 8*F*). In other parts of the retina, such as inner and outer nuclear layers, photoreceptors, and retinal pigment epitheliums, there were also no apparent changes.

## DISCUSSION

Blindness is a devastating consequence of PVDs such as PDR and PVR. Currently, the progression of these diseases cannot be effectively prevented, and the treatment options are limited to vitreoretinal surgery. An effective pharmacological treatment is thus urgently needed to complement or potentially replace the surgical intervention. In the current study, we show statins' novel function in inhibiting the Rho/Rho-kinase pathway, the contraction of collagen gel, and the progression of experimental PVR, suggesting the therapeutic potential of these compounds for the treatment of PVDs.

Various cytokines, such as TGF-β, connective tissue growth factor, interleukin-6, and platelet-derived growth factor (PDGF), are overexpressed in the vitreous and membranes associated with PDR and PVR, and they contribute to the pathogenesis of these diseases (15,37–40). Among these cytokines, TGF-β2 induces the transformation of retinal pigment epithelial cells or hyalocytes to myofibroblastic cells (18,41) and plays a key role in the formation and contraction of proliferative membranes. In this study, we confirmed the overexpression of TGF-β2 in the vitreous from patients with PVD (PDR and PVR) and showed that TGF-β2 inhibition strongly suppressed the vitreous-induced contraction of the collagen gels. This indicates the possibility that TGF-β2 is the dominant contributor to the contraction of proliferative membrane in the vitreous cavity. Thus, we focused on the role of TGF-β2 to investigate the mechanisms of membrane contraction. TGF-β2 enhanced MLC phosphorylation in hyalocytes that was responsible for the contraction of the hyalocyte-containing collagen gels. We showed that simvastatin suppressed TGF-β2–induced MLC phosphorylation and collagen gel contraction in a dose-dependent fashion by inhibiting GGPP-mediated translocation of Rho to the plasma membrane, whereas no signs of cytotoxicity were apparent.

Differences in the structural characteristics of statin cause different levels of lipophilicity and possibly of efficacies and also cytotoxicity. Pravastatin is strongly hydrophilic, and simvastatin is much more lipophilic than pravastatin (42). Fluvastatin is also more lipophilic than pravastatin; however, it is less lipophilic than simvastatin (43). Although our comparison of the inhibitory effects of various statins, simvastatin, fluvastatin, and pravastatin, revealed that simvastatin was more effective in reducing MLC phosphorylation than the other statins under the chosen experimental conditions, the results might vary at other time points or concentrations. Further examination is necessary to determine the order. Additionally, because cerivastatin is more lipophilic than simvastatin (44), we studied the effects of cerivastatin and simvastatin. Many hyalocytes treated with 5 μmol/l cerivastatin for 24 h shrank and detached from the culture plates, whereas the cells treated with 5 μmol/l simvastatin remained morphologically unchanged. However, at higher concentrations (>20 μmol/l), some hyalocyte shrinkage was observed even with simvastatin (data not shown). Cerivastatin is known to be cytotoxic and induce apoptosis (45). The morphological changes we observed in cerivastatin-treated hyalocytes in our study suggest that this drug may also be toxic to hyalocytes and promote their apoptosis. Because the lipophilicity of lovastatin is similar to that of simvastatin (42), we compared their effect and found the inhibitory effect of simvastatin on MLC phosphorylation and collagen gel contraction to be greater than that of 5 μmol/l lovastatin for 24 h (data not shown).

Vitreous samples from patients with PDR and PVR induced MLC phosphorylation and contraction of hyalocyte-containing collagen gels, which were effectively inhibited by simvastatin. It may appear surprising that not only vitreous samples from patients with PVD but also those from non-PVD patients induced MLC phosphorylation and collagen gel contraction. However, this might be explained by the fact that TGF-β2 is expressed in vitreous samples of patients with macular hole at high enough concentrations to induce the observed phenomena. The concentrations of TGF-β2 in vitreous samples from patients with PVD (PDR and PVR) were higher than in those from macular hole patients. Therefore, in a concentration-dependent manner, the inductions might be greater in the vitreous samples

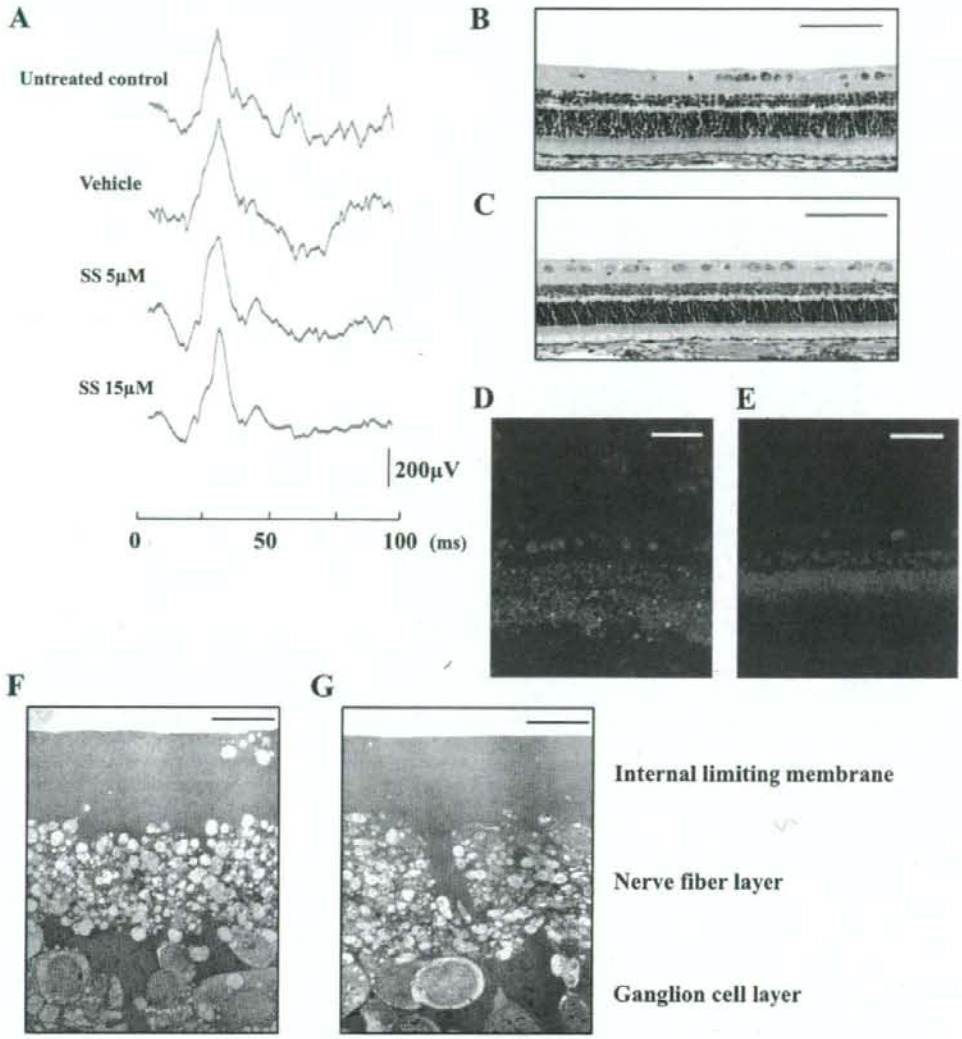


**FIG. 8. Histological and physiological examinations of eyes injected with simvastatin. Rabbits received intravitreal injections of 0.1 ml vehicle or vehicle with simvastatin (final concentration of 5 or 15 μmol/l simvastatin) on days 0, 1, 3, 5, and 7. *A*: Electroretinograms on day 28. A flash stimulus of intensity 1.30 log cd.s/m² was superimposed on a background luminance of 1.15 log cd/m². Light microscopy of the rabbit eye without any treatment (*B*) and that of the eye injected with 15 μmol/l simvastatin (*C*). Scale bar = 100 μm. Apoptotic and potentially necrotic cell death detected by TUNEL in the section from positive control (rabbit PVR model on day 7 after its onset) (*D*) and in the section from the 15 μmol/l simvastatin-treated eye (*E*). Scale bar = 50 μm. Transmission electron microscopy of the rabbit eye without treatment (*F*) and that of the eye injected with 15 μmol/l simvastatin (*G*). Scale bar = 10 μm. (Please see http://dx.doi.org/10.2337/db08-0302 for a high-quality digital representation of this image.)**

from patients with PVD than in those from patients without PVD. The concentrations of TGF-β2 in some vitreous samples from patients with macular hole were higher than those with PDR and PVR. However, the pathology of macular hole does not generally involve proliferative membrane formation and tractional retinal detachment. Occasionally, epiretinal membranes and retinal folds accompany macular hole. Retinal folds are considered to be caused by the contraction of the epiretinal membranes. TGF-β2 concentrations in vitreous samples from patients with macular hole may be high enough to induce contraction of proliferative membranes, however, because the epiretinal membrane in these patients does not extend into the vitreous and is very thin; the expression of TGF-β2 remains inconsequential.

MLC phosphorylation depends on the concentration of TGF-β2 (18); thus, the eyes with PVR having lower TGF-β2 concentrations might represent a less severe pathology, or remission, compared with those with higher TGF-β2 concentrations. The occurrence of tractional retinal detachment might depend on the presence or absence of proliferative membranes and the concentration of TGF-β2.

Although TGF-β2–stimulated hyalocytes showed no significant change in MLC expression, those stimulated with vitreous samples showed elevated MLC expression that was inhibited by simvastatin treatment. The vitreous in-

cludes various cytokines, released from retinal pigment epithelial cells, glial cells, macrophages, and other intravitreal cells (46). Thus, some cytokines other than TGF-β2 might elevate the expression of MLC. Among the cytokines found in the vitreous, insulin-like growth factor-I (IGF-I), PDGF, and members of the endothelin family have been shown to stimulate extracellular matrix contraction (18,47,48). This study reveals a key role for TGF-β2 in the pathology of PVDs; however, it is possible that other cytokines found in the vitreous might also be involved in MLC phosphorylation and contraction of hyalocyte-containing collagen gels. Because simvastatin almost completely inhibited the phenomena induced by vitreous samples, it might also inhibit the effect of the other cytokines, such as IGF-I, PDGF, and members of the endothelin family and unknowns, which might be exerted through the Rho/Rho-kinase pathway.

Simvastatin also prevented the development of PVR in vivo. Proliferative membranes in simvastatin-injected eyes, even if present, were very thin, whereas the membranes in vehicle injected eyes with PVR in stage 4 or 5 were thick. Thus, simvastatin might have also an inhibitory effect on the formation and growth of proliferative membranes in addition to the cicatricial contraction of proliferative membranes. However, after the end of the simvastatin injections, even in the groups treated with higher concentration of simvastatin (15 μmol/l) the development of PVR was not completely inhibited. This may be due to a short biological half-life time of the compound in the vitreous cavity. Therefore, to sustain a constant level of intravitreal simvastatin concentration, frequent injections or a slow release drug delivery system might be necessary.

Recent findings suggest that statins might have a number of beneficial effects in the eye. Although the applicability of statins on age-related macular degeneration is still under investigation (49), statins are shown to have protective effects on primary open-angle glaucoma, a major cause of blindness (50). The regulation of the intraocular pressure (IOP) within a physiological range is of great clinical importance. Statins are reported to downregulate the IOP by increasing aqueous humor outflow via the inhibition of Rho/Rho-kinase pathway in the trabecular meshwork and the ciliary body (50).

In conclusion, simvastatin potently inhibits the Rho/Rho-kinase pathway and thus might have therapeutic potential in the prevention of cicatricial contraction of proliferative membranes in vivo. This is the first report demonstrating the beneficial effects of simvastatin in inhibiting the development of PVR. Statins might provide a new strategy for the treatment and prevention of the development of PVDs in humans.

## ACKNOWLEDGMENTS

S.N. has received a Research Fellowship Award from Bausch & Lomb and a Fellowship Award from the Japan Eye Bank Association. A.H.-M. has received National Institutes of Health Grants AI050775 and HL086933. This study has received Grants-in-Aid for Scientific Research 19592026, 18791283, and 18591925 from the Ministry of Education, Science, Sports and Culture, Japan; National Eye Institute Core Grant EY14104; and support from the Massachusetts Lions Eye Research Fund, the Marion W. and Edward F. Knight Age-Related and Macular Degeneration Fund, and Research to Prevent Blindness.

We acknowledge David Goodman (Pharmascience), Waichiro Katsuda, Tomoko Saeki, and Noriyuki Yoshida (Aqumen Biopharmaceuticals) for their excellent help.

## REFERENCES

1. Pastor JC, de la Rua ER, Martin F: Proliferative vitreoretinopathy: risk factors and pathobiology. *Prog Retin Eye Res* 21:127–144, 2002
2. Pastor JC: Proliferative vitreoretinopathy: an overview. *Surv Ophthalmol* 43:3–18, 1998
3. Friedlander M: Fibrosis and diseases of the eye. *J Clin Invest* 117:576–586, 2007
4. Campochiaro PA: Pathogenic mechanisms in proliferative vitreoretinopathy. *Arch Ophthalmol* 115:237–241, 1997
5. Jerdan JA, Pepose JS, Michels RG, Hayashi H, de Bustros S, Sebag M, Glaser BM: Proliferative vitreoretinopathy membranes: an immunohistochemical study. *Ophthalmology* 96:801–810, 1989
6. Vinores SA, Campochiaro PA, Conway BP: Ultrastructural and electron-immunocytochemical characterization of cells in epiretinal membranes. *Invest Ophthalmol Vis Sci* 31:14–28, 1990
7. Machemer R, Laqua H: Pigment epithelium proliferation in retinal detachment (massive periretinal proliferation). *Am J Ophthalmol* 80:1–23, 1975
8. Lazarus HS, Hageman GS: In situ characterization of the human hyalocyte. *Arch Ophthalmol* 112:1356–1362, 1994
9. Grabner G, Boltz G, Forster O: Macrophage-like properties of human hyalocytes. *Invest Ophthalmol Vis Sci* 19:333–340, 1980
10. Mitchell CA, Risau W, Drexler HC: Regression of vessels in the tunica vasculosa lentis is initiated by coordinated endothelial apoptosis: a role for vascular endothelial growth factor as a survival factor for endothelium. *Dev Dyn* 213:322–333, 1998
11. Kampik A, Kenyon KR, Michels RG, Green WR, de la Cruz ZC: Epiretinal and vitreous membranes: comparative study of 56 cases. *Arch Ophthalmol* 99:1445–1454, 1981
12. Faulborn J, Dunker S, Bowald S: Diabetic vitreopathy: findings using the celloidin embedding technique. *Ophthalmologica* 212:369–376, 1998
13. Pfeffer BA, Flanders KC, Guerin CJ, Danielpour D, Anderson DH: Transforming growth factor beta 2 is the predominant isoform in the neural retina, retinal pigment epithelium-choroid and vitreous of the monkey eye. *Exp Eye Res* 59:323–333, 1994
14. Connor TB Jr, Roberts AB, Sporn MB, Danielpour D, Dart LL, Michels RG, de Bustros S, Enger C, Kato H, Lansing M: Correlation of fibrosis and transforming growth factor-beta type 2 levels in the eye. *J Clin Invest* 83:1661–1666, 1989
15. Kita T, Hata Y, Kano K, Miura M, Nakao S, Noda Y, Shimokawa H, Ishibashi T: Transforming growth factor-β2 and connective tissue growth factor in proliferative vitreoretinal diseases: possible involvement of hyalocytes and therapeutic potential of Rho kinase inhibitor. *Diabetes* 56:231–238, 2007
16. Ando A, Ueda M, Uyama M, Masu Y, Ito S: Enhancement of dedifferentiation and myoid differentiation of retinal pigment epithelial cells by platelet derived growth factor. *Br J Ophthalmol* 84:1306–1311, 2000
17. Vinores SA, Henderer JD, Mahlow J, Chiu C, Derevjanik NL, Larochelle W, Csaky C, Campochiaro PA: Isoforms of platelet-derived growth factor and its receptors in epiretinal membranes: immunolocalization to retinal pigmented epithelial cells. *Exp Eye Res* 60:607–619, 1995
18. Hirayama K, Hata Y, Noda Y, Miura M, Yamanaka I, Shimokawa H, Ishibashi T: The involvement of the rho-kinase pathway and its regulation in cytokine-induced collagen gel contraction by hyalocytes. *Invest Ophthalmol Vis Sci* 45:3896–3903, 2004
19. Jester JV, Ho-Chang J: Modulation of cultured corneal keratocyte phenotype by growth factors/cytokines control in vitro contractility and extracellular matrix contraction. *Exp Eye Res* 77:581–592, 2003
20. Molgaard J, von Schenck H, Olsson AG: Effects of simvastatin on plasma lipid, lipoprotein and apolipoprotein concentrations in hypercholesterolaemia. *Eur Heart J* 9:541–551, 1988
21. Graaf MR, Richel DJ, van Noorden CJ, Guchelaar HJ: Effects of statins and farnesyltransferase inhibitors on the development and progression of cancer. *Cancer Treat Rev* 30:609–641, 2004
22. MRC/BHF Heart Protection Study of cholesterol lowering with simvastatin in 20,536 high-risk individuals: a randomised placebo-controlled trial. *Lancet* 360:7–22, 2002
23. Coons JC: Hydroxymethylglutaryl-coenzyme A reductase inhibitors in osteoporosis management. *Ann Pharmacother* 36:326–330, 2002
24. Campbell MJ, Esserman LJ, Zhou Y, Shoemaker M, Lobo M, Borman E, Baehner F, Kumar AS, Adduci K, Marx C, Petricoin EF, Liotta LA, Winters M, Benz S, Benz CC: Breast cancer growth prevention by statins. *Cancer Res* 66:8707–8714, 2006

25. Matar P, Rozados VR, Binda MM, Roggero EA, Bonfil RD, Scharovsky OG: Inhibitory effect of Lovastatin on spontaneous metastases derived from a rat lymphoma. *Clin Exp Metastasis* 17:19–25, 1999
26. Van Aelst L, D'Souza-Schorey C: Rho GTPases and signaling networks. *Genes Dev* 11:2295–2322, 1997
27. Laufs U, Liao JK: Post-transcriptional regulation of endothelial nitric oxide synthase mRNA stability by Rho GTPase. *J Biol Chem* 273:24266–24271, 1998
28. Hall A: Rho GTPases and the actin cytoskeleton. *Science* 279:509–514, 1998
29. Paterson HF, Self AJ, Garrett MD, Just I, Aktories K, Hall A: Microinjection of recombinant p21rho induces rapid changes in cell morphology. *J Cell Biol* 111:1001–1007, 1990
30. Takaishi K, Sasaki T, Kato M, Yamochi W, Kuroda S, Nakamura T, Takeichi M, Takai Y: Involvement of Rho p21 small GTP-binding protein and its regulator in the HGF-induced cell motility. *Oncogene* 9:273–279, 1994
31. Kureishi Y, Kobayashi S, Amano M, Kimura K, Kanaide H, Nakano T, Kaibuchi K, Ito M: Rho-associated kinase directly induces smooth muscle contraction through myosin light chain phosphorylation. *J Biol Chem* 272:12257–12260, 1997
32. Amano M, Chihara K, Kimura K, Fukata Y, Nakamura N, Matsuura Y, Kaibuchi K: Formation of actin stress fibers and focal adhesions enhanced by Rho-kinase. *Science* 275:1308–1311, 1997
33. Noda Y, Hata Y, Hisatomi T, Nakamura Y, Hirayama K, Miura M, Nakao S, Fujisawa K, Sakamoto T, Ishibashi T: Functional properties of hyalocytes under PDGF-rich conditions. *Invest Ophthalmol Vis Sci* 45:2107–2114, 2004
34. Dong X, Chen N, Xie L, Wang S: Prevention of experimental proliferative vitreoretinopathy with a biodegradable intravitreal drug delivery system of all-trans retinoic acid. *Retina* 26:210–213, 2006
35. Fastenberg DM, Diddie KR, Dorey K, Ryan SJ: The role of cellular proliferation in an experimental model of massive periretinal proliferation. *Am J Ophthalmol* 93:565–572, 1982
36. Ito S, Sakamoto T, Tahara Y, Goto Y, Akazawa K, Ishibashi T, Inomata H: The effect of tranilast on experimental proliferative vitreoretinopathy. *Graefes Arch Clin Exp Ophthalmol* 237:691–696, 1999
37. Robbins SG, Mixon RN, Wilson DJ, Hart CE, Robertson JE, Westra I, Planck SR, Rosenbaum JT: Platelet-derived growth factor ligands and receptors immunolocalized in proliferative retinal diseases. *Invest Ophthalmol Vis Sci* 35:3649–3663, 1994
38. Hinton DR, Spee C, He S, Weitz S, Usinger W, LaBree L, Oliver N, Lim JI: Accumulation of $NH_2$-terminal fragment of connective tissue growth factor in the vitreous of patients with proliferative diabetic retinopathy. *Diabetes Care* 27:758–764, 2004
39. Hinton DR, He S, Jin ML, Barron E, Ryan SJ: Novel growth factors involved in the pathogenesis of proliferative vitreoretinopathy. *Eye* 16:422–428, 2002
40. Kauffmann DJ, van Meurs JC, Mertens DA, Peperkamp E, Master C, Gerritsen ME: Cytokines in vitreous humor: interleukin-6 is elevated in proliferative vitreoretinopathy. *Invest Ophthalmol Vis Sci* 35:900–906, 1994
41. Gamulescu MA, Chen Y, He S, Spee C, Jin M, Ryan SJ, Hinton DR: Transforming growth factor beta2-induced myofibroblastic differentiation of human retinal pigment epithelial cells: regulation by extracellular matrix proteins and hepatocyte growth factor. *Exp Eye Res* 83:212–222, 2006
42. Serajuddin AT, Ranadive SA, Mahoney EM: Relative lipophilicities, solubilities, and structure-pharmacological considerations of 3-hydroxy-3-methylglutaryl-coenzyme A (HMG-CoA) reductase inhibitors pravastatin, lovastatin, mevastatin, and simvastatin. *J Pharm Sci* 80:830–834, 1991
43. Hamelin BA, Turgeon J: Hydrophilicity/lipophilicity: relevance for the pharmacology and clinical effects of HMG-CoA reductase inhibitors. *Trends Pharmacol Sci* 19:26–37, 1998
44. Chauhan NB, Siegel GJ, Feinstein DL: Effects of lovastatin and pravastatin on amyloid processing and inflammatory response in TgCRND8 brain. *Neurochem Res* 29:1897–1911, 2004
45. Kobayashi M, Kaido F, Kagawa T, Itagaki S, Hirano T, Iseki K: Preventive effects of bicarbonate on cerivastatin-induced apoptosis. *Int J Pharm* 341:181–188, 2007
46. El-Ghrably IA, Dua HS, Orr GM, Fischer D, Tighe PJ: Intravitreal invading cells contribute to vitreal cytokine milieu in proliferative vitreoretinopathy. *Br J Ophthalmol* 85:461–470, 2001
47. Guidry C, Hook M: Endothelins produced by endothelial cells promote collagen gel contraction by fibroblasts. *J Cell Biol* 115:873–880, 1991
48. Guidry C: Tractional force generation by porcine Muller cells: development and differential stimulation by growth factors. *Invest Ophthalmol Vis Sci* 38:456–468, 1997
49. Wilson HL, Schwartz DM, Bhatt HR, McCulloch CE, Duncan JL: Statin and aspirin therapy are associated with decreased rates of choroidal neovascularization among patients with age-related macular degeneration. *Am J Ophthalmol* 137:615–624, 2004
50. Song J, Deng PF, Stinnett SS, Epstein DL, Rao PV: Effects of cholesterol-lowering statins on the aqueous humor outflow pathway. *Invest Ophthalmol Vis Sci* 46:2424–2432, 2005

Jpn J Ophthalmol 2008;52:16–23
© Japanese Ophthalmological Society 2008

DOI 10.1007/s10384-007-0487-5

LABORATORY INVESTIGATION

# Antiangiogenic Properties of Fasudil, a Potent Rho-kinase Inhibitor

Yasuaki Hata, Muneki Miura, Shintaro Nakao, Shuhei Kawahara, Takeshi Kita, and Tatsuro Ishibashi

Department of Ophthalmology, Graduate School of Medical Sciences, Kyushu University, Fukuoka, Japan

**Abstract**

**Purpose:** Vascular endothelial growth factor (VEGF) plays a pivotal role in pathological angiogenesis. In this study, we addressed the therapeutic potential of fasudil, a potent Rho-kinase inhibitor, for VEGF-elicited angiogenesis and also for the intracellular signalings induced by VEGF.

**Methods:** In vitro, the inhibitory effects of fasudil on the VEGF-dependent VEGF receptor 2 (VEFGR2 or KDR), extracellular signal-related kinase (ERK) 1/2, Akt and myosin light chain (MLC) phosphorylation, as well as on the migration and proliferation of bovine retinal microvascular endothelial cells (BRECs) were analyzed with Western blotting, [$^3$H]-thymidine uptake, and modified Boyden chamber assay. VEGF-elicited in vivo angiogenesis was analyzed with a mouse corneal micropocket assay coembedded with or without fasudil.

**Results:** VEGF caused enhanced MLC phosphorylation of BRECs, which was almost completely attenuated by 10μM fasudil. VEGF-dependent phosphorylation of ERK1/2 and Akt were also partially but significantly attenuated by treatment with fasudil without affecting VEGFR2 (KDR) phosphorylation. Moreover, both VEGF-induced [$^3$H]-thymidine uptake and the migration of BRECs were significantly inhibited in the presence of fasudil. Finally, VEGF-elicited angiogenesis in the corneal micropocket assay was potently attenuated by coembedding with fasudil ($P < 0.01$).

**Conclusions:** These findings indicate that fasudil might have a therapeutic potential for ocular angiogenic diseases. The antiangiogenic effect of fasudil appears to be mediated through the blockade not only of Rho-kinase signaling but also of ERK and Akt signaling. **Jpn J Ophthalmol** 2008;52:16–23
© Japanese Ophthalmological Society 2008

**Key Words:** angiogenesis, myosin light chain phosphorylation, retina, Rho-kinase, vascular endothelial growth factor

## Introduction

The small GTPase RhoA and its downstream effector, Rho-kinase, play a central role in diverse cellular functions, including smooth muscle contraction, cytoskeletal rearrangement, cell migration, cell proliferation and gene expression.[1] As pharmacological inhibitors of Rho-kinase, fasudil[2] and Y-27632[3] have inhibitory Rho-kinase activity in a competitive manner with ATP. Accumulating evidence from animal and clinical studies indicates that Rho-kinase inhibitors have broad pharmacological properties for treating various diseases, including cardiovascular and renal diseases.[1]

In the pathogenesis of proliferative diabetic retinopathy, neovascularization is regulated by various growth factors and cytokines, especially by hypoxia-inducible vascular endothelial growth factor (VEGF), which regulates endothelial cell proliferation, migration, and permeability, and by the adhesive contacts of endothelial cells with the extracellular matrix.[4,5]

Received: March 12, 2007 / Accepted: September 15, 2007
Correspondence and reprint requests to: Yasuaki Hata, Department of Ophthalmology, Graduate School of Medical Sciences, Kyushu University, 3-1-1 Maidashi, Higashi-Ku, Fukuoka 812-8582, Japan
e-mail: hatachan@med.kyushu-u.ac.jp

During the last several years, a number of therapeutic agents, such as bevacizumab (Avastin, Genentech, South San Francisco, CA, USA), a monoclonal antibody that binds to human VEGF with high affinity, and pegaptanib sodium (Macugen, Eyetech Pharmaceuticals, New York, NY, USA; and Pfizer, New York, NY, USA), an anti-VEGF aptamer that specifically blocks the 165 isoform of VEGF, have been investigated for their efficacy in the pharmacological treatment of intraocular neovascularization.[6,7] Moreover, many products, such as alpha-defensins, VEGF165b (an endogenous C-terminal splice variant of VEGF), Ephrin A1, and vasohibin, have been reported to suppress retinal angiogenesis.[8-11]

VEGF is essential for various angiogenic processes. The binding of VEGF to its cognate receptors induces dimerization and subsequent phosphorylation of the receptors, leading to activation of several intracellular signaling molecules such as phosphatidylinositol 3-kinase/Akt, and mitogen-activated protein kinases (MAPKs).[12]

Rho-kinase is reported to be implicated in endothelial cell migration, which is an essential step for angiogenesis.[13,14] The initial event in cell migration is polarization and extension of protrusions in the direction of migration. Rho-kinase controls the formation of these prominences (lamellipodia and filopodia) by regulating the cytoskeleton and cell adhesion.[15] In endothelial cells Rho-kinase regulates stress fiber formation and cell–cell junctions in response to VEGF,[13,16] which might be associated with the phosphorylation of the myosin light chain (MLC), a target protein of Rho-kinase.[17] Moreover, recent in vivo studies have demonstrated that the Rho/Rho-kinase pathway plays a critical role in angiogenesis.[18,19]

In the clinic, fasudil, a potent Rho-kinase inhibitor, is effective for the treatment of a wide range of cardiovascular diseases, including cerebral and coronary vasospasm, angina, hypertension, pulmonary hypertension, and heart failure, with reasonable safety.[20-23] Rho-kinase is thus an important therapeutic target in cardiovascular medicine today. In the present study, we first demonstrated that fasudil could inhibit VEGF-elicited bovine retinal endothelial cell (BREC) migration and proliferation, and corneal neovascularization, possibly by suppressing both extracellular signal-related kinase (ERK) 1/2 and Akt phosphorylation involved in cell survival and migration[24,25] in addition to Rho-kinase activity.

## Materials and Methods

### *Materials*

Recombinant human $VEGF_{165}$ and recombinant mouse $VEGF_{164}$ were purchased from R & D Systems (Minneapolis, MN, USA). Goat polyclonal antibodies against MLC and phosphorylated MLC (pMLC) were obtained from Santa Cruz Biotech (Santa Cruz, CA, USA). A specific Rho-kinase inhibitor, Y-27632, was obtained from Calbiochem (San Diego, CA, USA). Fasudil, a potent Rho-kinase inhibitor, was generously provided by Asahi Kasei, Tokyo, Japan. Anti-phospho-p44/42 MAPK ($Thr^{202}/Tyr^{204}$) E10 mouse monoclonal antibody and phospho-Akt ($Thr^{308}$) and anti-total Akt rabbit polyclonal antibodies were purchased from Cell Signaling Technology (Beverly, MA, USA). Rabbit polyclonal antibody against Flk-1/KDR (VEGF receptor 2; VEGFR2) agarose conjugate (C-1158; SC-504AC), Flk-1/KDR (A-3; SC-6251) and ERK1 (K-23; SC-94) were obtained from Santa Cruz Biotech. Mouse monoclonal anti-phosphotyrosine (clone PY20) antibody was obtained from MP Biomedicals (Aurora, OH, USA).

### *Cell Culture*

Isolated BRECs from eyes of freshly killed cattle were primarily cultured on a fibronectin-coated dish. Thereafter, typical cobblestone cells were selected and cultured on a type 1 collagen-coated dish up to passage 9 in Humedia-EB2 supplemented with Humedia-EG [2% fetal bovine serum (FBS), human epidermal growth factor (10 ng/ml), hydrocortisone (10 μg/ml), heparin (10 μg/ml), gentamicin (50 μg/ml), and amphotericin-B (50 ng/ml)] (Kurabo, Osaka, Japan) and 5% heat-inactivated horse serum (Sigma Chemical, St. Louis, MO, USA) at 37°C in a humidified 5% $CO_2$ atmosphere.

### *Western Blot Analysis*

BRECs were incubated up to a 90% confluent state and starved in Dulbecco's modified Eagle medium (DMEM, Gibco, Grand Island, NY, USA) supplemented with 3% heat-inactivated bovine serum (BS, Gibco) for 24 h. After incubation in the presence or absence of fasudil (10 μM) for 30 min, cells were stimulated with human VEGF (25 ng/ml) and mechanically scraped for collection. Equal amounts of total cell lysates or immunoprecipitated KDR were separated on sodium dodecyl sulfate-polyacrylamide gels and transferred to nitrocellulose membranes. The blots were blocked with skimmed milk and incubated overnight at 4°C with primary antibodies (1 : 1000). After being washed three times for 10 min each time with t-TBS (20 mM Tris, pH 7.5; 500 mM NaCl; and 0.1% Tween-20), the membranes were incubated with horseradish peroxidase-labeled antibodies (Bio-Rad, Richmond, CA, USA), 1 : 4000 for 30 min at room temperature. Visualization was performed with an enhanced chemiluminescence (Amersham, Arlington Heights, IL, USA) detection system according to the manufacturer's protocol.

### *Migration Assay*

BREC migration was measured by using modified Boyden chambers with 8-μm-pore filters (Kurabo), as previously described.[26] Briefly, BRECs were suspended at a density of $3 \times 10^5$ cells/ml with 1% BS DMEM with or without

fasudil (10μM), and 300μl of the suspensions were seeded on the fibronectin-coated upper chambers. Then, the upper chambers were inserted into the lower wells of 24-well plates filled with 700μl of 1% BS DMEM, if needed, containing human VEGF (25ng/ml). After 4h of culture, the BRECs located on the top surfaces of the transwells were scraped off with cotton swabs, fixed in 70% ethanol, and stained with Giemsa's solution for 1h. After the meshes were punched out, BRECs on the bottom surfaces of the meshes were counted at predefined positions under a microscope.

### *[$^3$H]-Thymidine Uptake*

BRECs were seeded into 24-well plates at a density of $1.0 \times 10^4$ cells/well. The media were replaced by DMEM with 3% FBS the next day. After 24h, the cells were stimulated with human VEGF (25ng/ml) for 18h with or without fasudil (10μM). [$^3$H]-thymidine was then added (0.25μCi/well) for an additional 6h, after which the cells were washed, fixed, and lysed. Incorporated [$^3$H]-thymidine was determined by scintillation counting, as previously described.[26]

### *Immunoprecipitation*

Immunoprecipitation was performed as described below; 500μl of whole cell lysate was added with 500μl of 1% NP-40 lysis buffer (2% TritonX-100, 300mM NaCl, 20mM Tris pH 7.4, 1% Nonidet P-40, 2mM EDTA, 2mM EGTA, 0.4mM sodium orthovanadate, 0.4mM phenylmethylsulfonyl fluoride), and 5μg of rabbit polyclonal anti-Flk-1/KDR antibody agarose conjugate, and then incubated at 4°C overnight with mixing. Pellets, collected by centrifugation at 4000*g*, were washed three times with 0.5% NP-40 lysis buffer and resuspended in 60μl of 4× electrophoresis sample buffer. After boiling for 5min, samples were subjected to Western blotting.

### *Corneal Micropocket Assay in Mice*

All animal experiments were approved by the Committee on the Ethics of Animal Experiments, Kyushu University Graduate School of Medical Sciences, Japan. Male BALB/c mice (6–10 weeks old) were purchased from Seac Yoshitomi (Fukuoka, Japan) and anesthetized with pentobarbital sodium (60mg/kg intraperitoneally). Hydron pellets (0.3μl) (IFN Sciences, New Brunswick, NJ, USA) containing 200ng mouse VEGF and with or without fasudil (750ng/pellet) were prepared and implanted into the corneas. After 6 days, images of the corneal vessels were recorded by using Viewfinder 3.0 (Pixera), with standardized illumination and contrast, and were saved onto disks. Quantitative analysis of neovascularization in the mouse corneas was performed with the NIH image software package.[27]

### *Statistical Analysis*

The experimental data are expressed as means ± SD. Statistical significance was assumed when results showed $P < 0.05$, using the Student $t$ test in a normally distributed population.

## Results

### *Phosphorylation State of MLC in the Presence of VEGF*

To examine the effect of VEGF on MLC phosphorylation in BRECs, we assessed the time course of MLC phosphorylation in VEGF-stimulated BRECs with Western blotting. As shown in Fig. 1A, VEGF transiently dephosphorylated MLC within 5min (48.2 ± 19.7%; $^{**}P < 0.01$) and then sequentially increased the phosphorylated state of MLC (201 ± 6.63% at 60min; $^{**}P < 0.01$).

### *Inhibitory Potential of Fasudil on MLC Phosphorylation in Endothelial Cells*

The phosphorylation state of MLC is increased when endothelial cells start stretching to remodel the vascular network.[28] To examine whether fasudil could inhibit the activation of Rho-kinase in BRECs, we examined the phosphorylation state of MLC with Western blotting. We first examined dose-dependent inhibitory effects of fasudil on MLC phosphorylation under 10% serum conditions. The phosphorylation state of MLC was almost completely inhibited within 30min by fasudil treatment at a concentration of 10μM (2.91 ± 1.00% versus 0μM, $^{*}P < 0.01$). Moreover, pretreatment with fasudil for 30min strongly suppressed the phosphorylation state of MLC induced by VEGF (4.66 ± 2.53% versus VEGF alone; $^{**}P < 0.01$) (Fig. 1B, C).

### *Fasudil Attenuated VEGF-Dependent Migration of BRECs*

We investigated the effect of fasudil on endothelial cell migration by using a modified Boyden chamber assay. VEGF induced BREC migration markedly, and the effect was significantly attenuated by fasudil. The number of cells in the VEGF-stimulated group was markedly increased compared with the vehicle-treated group (vehicle alone, 95.2 ± 18.1 cells/field; VEGF alone, 326 ± 56.0 cells/field). However, VEGF-dependent BREC migration was significantly inhibited in the presence of 10μM fasudil (VEGF alone, 326 ± 56.0 cells/field; VEGF with fasudil, 79.0 ± 15.8 cells/field). (Fig. 2A, B) We also confirmed the inhibitory effect of fasudil on VEGF-induced BREC migration in a scratch wound assay, and the results were consistent with those of the Boyden chamber assay (data not shown).

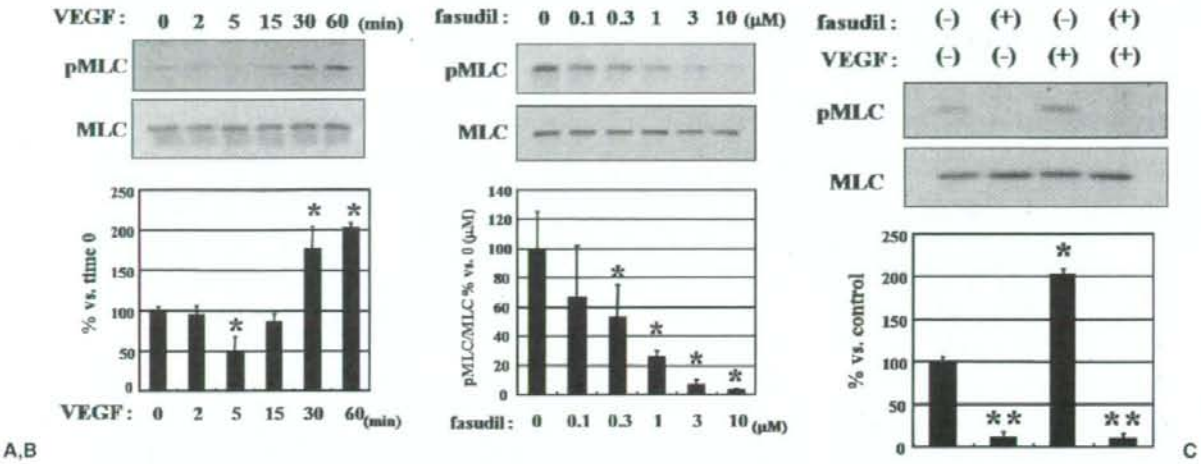


**Figure 1A–C.** Vascular endothelial growth factor (*VEGF*)-dependent phosphorylation of the myosin light chain (*MLC*) and the inhibitory effect of fasudil. **A** Bovine retinal endothelial cells (BRECs) were incubated in 3% bovine serum (BS)/Dulbecco's modified Eagle medium (DMEM) for 24h and then stimulated with human VEGF (25ng/ml) for the indicated time. Representative immunoblots for MLC phosphorylation (*pMLC*) and total MLC are shown. Values are means ± SD from three independent experiments. $^{*}P < 0.01$ versus time 0. **B** BRECs incubated in 3% BS DMEM for 24h were further incubated with (0.1–10μM) or without fasudil for 30min. Typical immunoblots for pMLC and total MLC are shown. Values are means ± SD from three independent experiments. $^{*}P < 0.01$ versus 0μM. **C** BRECs were incubated in 3% BS DMEM for 24h and then treated with vehicle or 10μM fasudil, and stimulated with human VEGF (25ng/ml) for 60min. Values are means ± SD from three independent experiments. $^{*}P < 0.01$; $^{**}P < 0.01$ versus each control.

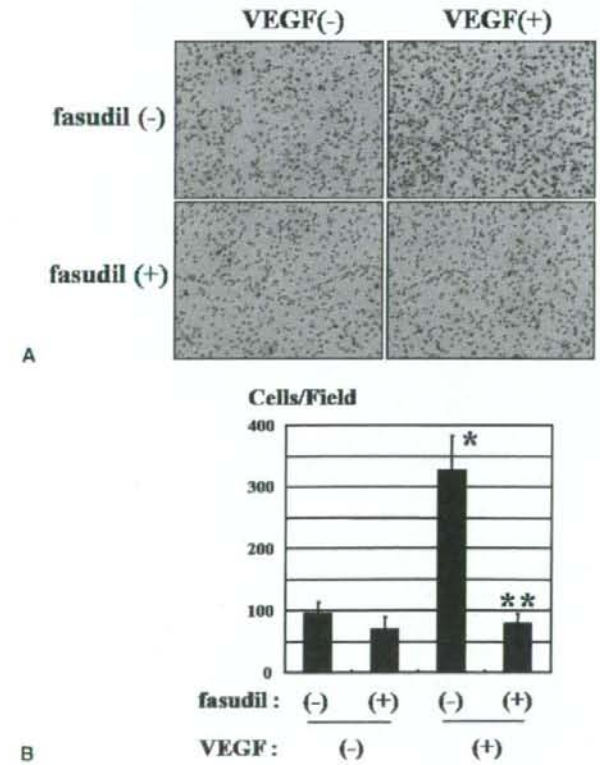


**Figure 2A,B.** VEGF-dependent migration of BRECs. **A** BREC migration was measured by using modified Boyden chambers with 8-μm-pore filters. After 4h of culture with or without human VEGF (25ng/ml), BRECs on the bottom surfaces of the mesh were photographed. **B** Transmigrated BRECs on the bottom surfaces of the mesh were counted at predefined positions under a microscope and quantified. Values are means ± SD from six cultures. $^{*}P < 0.01$ versus vehicle alone, $^{**}P < 0.01$ versus VEGF alone.

### *BREC Thymidine Uptake Induced by VEGF Was Inhibited by Fasudil*

It has been unclear whether Rho-kinase inhibition suppresses VEGF-induced endothelial cell proliferation. To examine whether treatment by fasudil affected de novo DNA synthesis in BRECs, we examined the effect of fasudil on thymidine uptake, an index of proliferation. We confirmed that thymidine uptake was promoted by VEGF (135.0 ± 14.3% versus control) and that fasudil inhibited thymidine uptake in a dose-dependent manner (data not shown). In BRECs treated with 10μM fasudil, mean thymidine uptake induced by VEGF was significantly reduced (74.07 ± 6.34% versus VEGF alone) (Fig. 3).

### *Fasudil Had No Inhibitory Effect on VEGF Receptor-2 (KDR) Phosphorylation*

VEGF signaling in endothelial cells is mainly mediated via KDR.[12] To investigate the selectivity of the inhibitory effect of fasudil on Rho-kinase activation, the phosphorylation state of KDR was assessed by Western blot analysis. We observed that KDR was phosphorylated by VEGF and that the phosphorylation state of KDR was not significantly affected by fasudil (Fig. 4A).

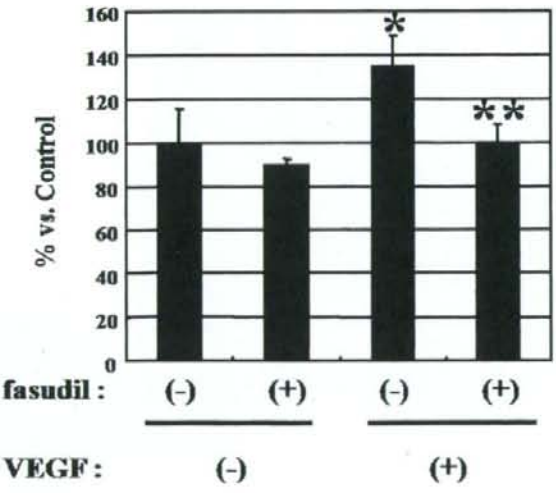


**Figure 3.** Inhibitory effect of fasudil on VEGF-induced thymidine uptake by BRECs. BRECs were seeded on a type 1 collagen-coated 24-well plate. The media were replaced by DMEM with 3% fetal bovine serum the next day. After 24h, the cells were stimulated with human VEGF (25ng/ml) for 18h with or without fasudil (10μM). [$^3$H]-thymidine was then added (0.25μCi/well) for an additional 6h, after which the cells were washed, fixed, and lysed. Incorporated [$^3$H]-thymidine was determined by scintillation counting. $^*P < 0.01$ versus vehicle alone; $^{**}P < 0.01$ versus VEGF alone.

### *Fasudil Inhibited VEGF-Induced Phosphorylation of ERK1/2 and Akt*

To investigate the inhibitory mechanisms of VEGF-induced angiogenesis by fasudil, we examined the effect of fasudil on the signal transduction by VEGF in BRECs. VEGF is known to activate ERK1/2 and Akt in endothelial cells during angiogenesis.[12,29] By Western blotting, we investigated which signaling pathway fasudil affected in VEGF-induced angiogenesis. VEGF induced the phosphorylation of ERK1/2, and the phosphorylation was partly inhibited by fasudil (Fig. 4B). We also examined whether fasudil inhibited VEGF-induced Akt phosphorylation. Fasudil significantly inhibited VEGF-induced phosphorylation of Akt in BRECs (Fig. 4C).

### *Fasudil Inhibited VEGF-elicited Angiogenesis in a Corneal Pocket Assay*

The mouse cornea is a useful organ for estimation of angiogenesis because of its avascular character.[27] To examine whether fasudil could inhibit VEGF-induced angiogenesis in vivo, we implanted VEGF-embedded pellets into mouse corneas. VEGF-induced corneal neovascularization was almost completely inhibited by coembedding mouse VEGF and fasudil in the pocket (11.1% versus VEGF alone) (Fig. 5A, B). These results showed fasudil to be a potent inhibitor of VEGF-dependent angiogenesis in vivo.

## Discussion

Accumulating evidence, obtained using the specific Rho-kinase inhibitor Y-27632, demonstrates that the Rho/Rho-kinase pathway plays a crucial role in cell migration.[13,14] However, few studies have examined the participation of the Rho-kinase pathway in ocular angiogenesis, and this is the first report indicating the inhibitory potency of fasudil on ocular angiogenesis in retinal microvascular endothelial cells.

Fasudil markedly attenuated VEGF-induced BREC migration in the Boyden chamber assay, and this inhibitory effect was in parallel with the phosphorylation state of MLC. Additionally, we confirmed the inhibitory effect of fasudil on BREC migration with a scratch wound assay, and the result was similar to that of the Boyden chamber assay (data not shown). Consistent with previous data concerning Y-27632 (10μM), in the scratch wound motility assay, fasudil (10μM) inhibited VEGF-dependent BREC migration almost completely, but not basal migration, without affecting cell viability (data not shown).

Endothelial cell proliferation is also an essential process for angiogenesis. In this study, fasudil significantly inhibited VEGF-induced BREC [$^3$H]-thymidine incorporation and ERK1/2 phosphorylation, whose activity indicates the proliferative activities of endothelial cells in angiogenic processes.[29]

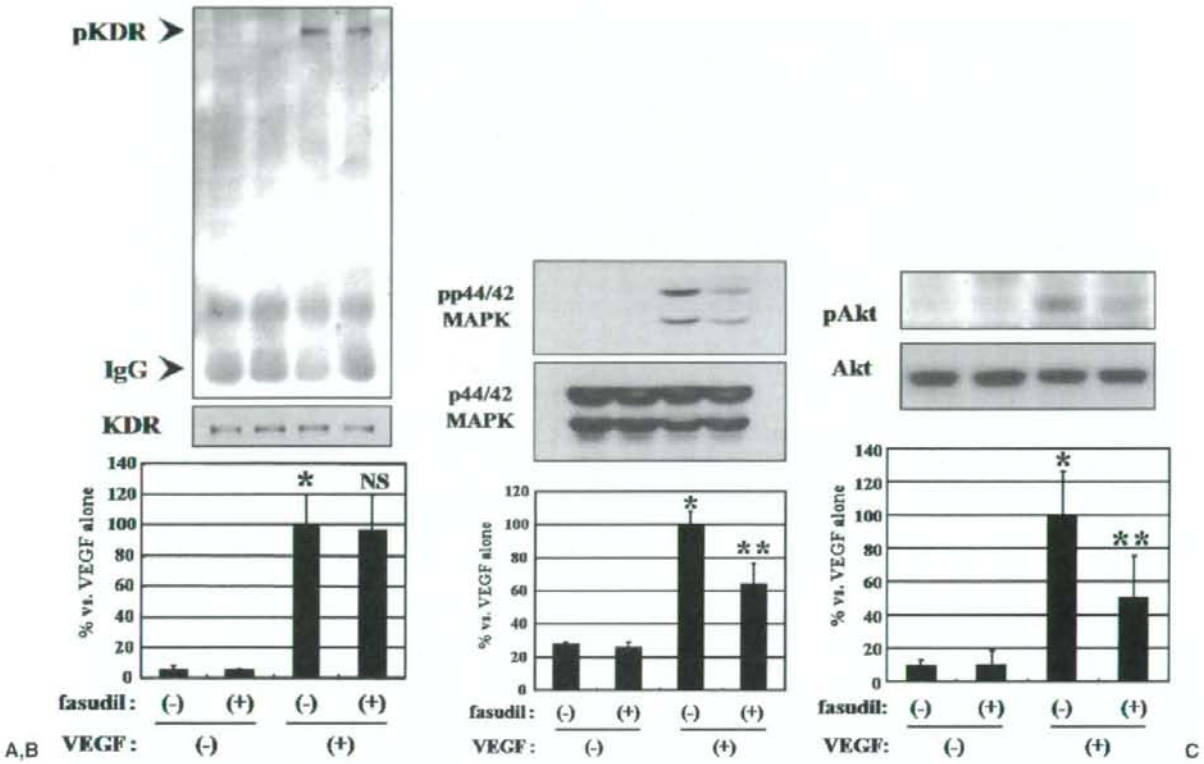


**Figure 4A–C.** Effect of fasudil on VEGF-dependent VEGF receptor 2 (*KDR*), extracellular signal-related kinase (ERK) 1/2 [*p44/42* mitogen-activated protein kinase (*MAPK*)] and Akt phosphorylation. **A** After pretreatment with fasudil (10 μM), BRECs stimulated with human VEGF (25 ng/ml) for 5 min were lysed, and immunoprecipitated KDR were loaded on a 6% sodium dodecyl sulfate polyacrylamide gel; an anti-phosphor-tyrosine antibody (PY-20) was used for detection of phosphorylated KDR (*pKDR*). Values are means ± SD from three independent experiments. $^{*}P < 0.01$ versus control; *NS*, not significant versus VEGF alone. **B, C** After pretreatment with fasudil (10 μM) or vehicle for 30 min, BRECs stimulated with human VEGF (25 ng/ml) for 5 min were lysed and subjected to Western blotting. The phosphorylated state of phosphorylated ERK1/2 (*pp44/42 MAPK*) or Akt was detected by immunoblot analysis (*top*). Both membranes were reblotted with anti-ERK1/2 or Akt antibody (*bottom*). Values are means ± SD from three independent experiments. $^{*}P < 0.01$ versus control; $^{**}P < 0.01$ versus VEGF alone.

Mavria et al.[30] reported that ERK–MAPK promotes endothelial cell survival and sprouting by downregulation of Rho-kinase signaling. They demonstrated that the blockade of angiogenesis by inhibition of ERK1/2 signaling was overcome by the Rho-kinase inhibitor Y-27632. Their results suggest that the Rho-kinase inhibitor might allow endothelial cells to sprout, leading to neovascularization. Therefore, there might be alternative possibilities concerning the effect of fasudil on angiogenic processes. In fact, fasudil strongly attenuated VEGF-induced corneal neovascularization. Our study using BRECs demonstrated that lysophosphatidic acid (LPA), an agonist of the Rho-kinase pathway, affected neither ERK1/2 nor Akt phosphorylation (data not shown). On the other hand, phosphomolybdic acid (PMA), which caused ERK1/2 phosphorylation in BRECs, did not affect the phosphorylation state of MLC, which is one of the downstream mediators of the Rho-kinase pathway (data not shown). Nevertheless, fasudil significantly suppressed not only Rho-kinase but also ERK1/2 signaling pathways. The interplay between Rho-kinase and ERK1/2 signaling thus seems to be independent in BRECs. Moreover, we verified that PMA induced Akt phosphorylation in a time-dependent manner in BRECs (data not shown), a finding that is consistent with previous reports that VEGF induces protein kinase C-dependent Akt phosphorylation in human umbilical vein endothelial cells.[31] On the other hand, LPA had no apparent effect on the phosphorylation state of Akt (data not shown). Our study provides evidence that the antiangiogenic effect of fasudil in VEGF-induced angiogenesis may be mediated independently by the blockade of Rho-kinase, ERK1/2, and Akt signaling.

At a concentration of 10 μM, fasudil is known to be relatively selective for Rho-kinase and to have minimal effects on other signaling pathways, such as MLC kinase and protein kinase C.[32] Furthermore, Y-27632, another Rho-

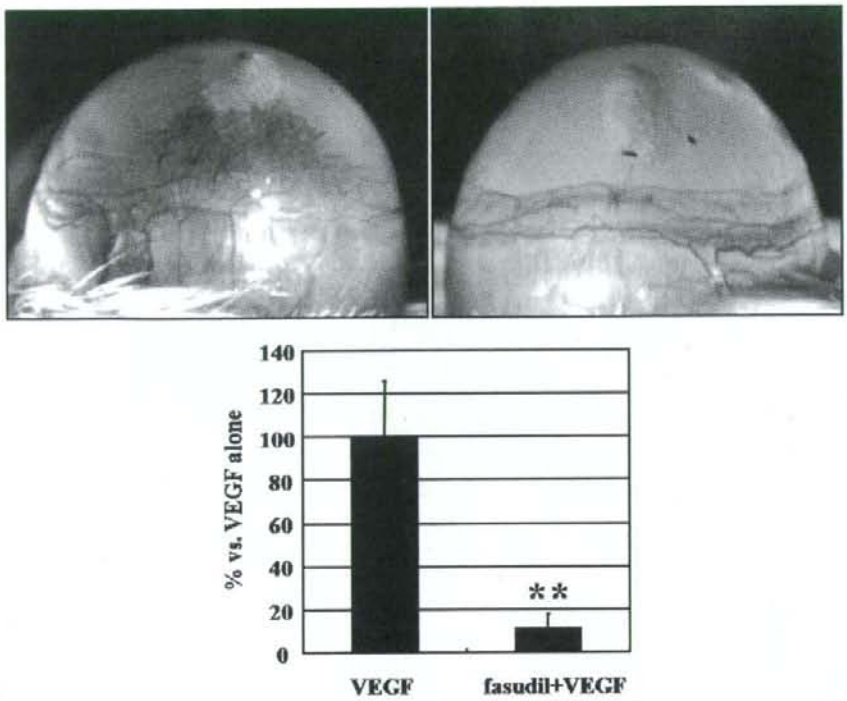


**Figure 5A,B.** In vivo antiangiogenic effect of fasudil. **A** 0.3 μl Hydron pellets containing 200 ng mouse VEGF with or without fasudil (750 ng/pellet) were prepared and implanted into the corneas of BALB/c mice. After 6 days, images of the corneal vessels were recorded with standardized illumination and contrast. Two representative *photographs* are shown. **B** Two quantitative analyses of corneal neovascularization on day 6. Coimplantation of fasudil inhibited VEGF-induced angiogenesis ($n = 12$ each). $^{**}P < 0.01$ versus VEGF alone-implanted mice.

kinase inhibitor, had similar effects on the inhibition of ERK1/2 signaling, but not on Akt phosphorylation (data not shown), suggesting that fasudil has a broader and more suppressive effect than Y27632 on the migration or survival of retinal endothelial cells, whereas Wolfrum et al.[33] observed that 10 μM fasudil slightly increased Akt phosphorylation in human microvascular endothelial cells. The differences in additional effects in each type of endothelial cells will require further examination.

Finally, we examined whether fasudil could suppress VEGF-induced in vivo neovascularization in a corneal pocket assay. Fasudil strongly attenuated VEGF-induced angiogenesis with no apparent adverse effects such as corneal edema or inflammation. However, the effective concentration of fasudil on angiogenesis in vivo was not estimated, since the concentration of fasudil in the tissue surrounding the pellet could not be measured precisely in this study. Further investigation in vivo is thus needed to determine the clinically efficient and safe use of fasudil.

Our previous reports also demonstrated that Rho-kinase inhibition by fasudil might have therapeutic potential for the prevention of proliferative vitreoretinal diseases.[34,35] However, pharmacological treatment sometimes leads to undesirable side effects in vivo. Further in vivo examination, therefore, is necessary to evaluate the therapeutic potential and safety of fasudil for clinical use in ocular diseases.

*Acknowledgments.* We thank Dr. Tadahisa Kagimoto, Michiyo Takahara, and Fumie Doi, at the Department of Ophthalmology, Kyushu University Graduate School of Medical Sciences, for their excellent help. We also thank Asahi Kasei Pharma Corporation, Tokyo, Japan, for the generous provision of fasudil. The study was supported in part by grants from the Ministry of Education, Culture, Sports, Science, and Technology of Japan (Grant-in-Aid for Scientific Research #19592026).

## References

1. Shimokawa H, Takeshita A. Rho-kinase is an important therapeutic target in cardiovascular medicine. Arterioscler Thromb Vasc Biol 2005;25:1767–1775.
2. Asano T, Ikegaki I, Satoh S, et al. Mechanism of action of a novel antivasospasm drug, HA1077. J Pharmacol Exp Ther 1987;24: 1033–1040.
3. Uehata M, Ishizaki T, Satoh H, et al. Calcium sensitization of smooth muscle mediated by a Rho-associated protein kinase in hypertension. Nature 1997;389:990–994.
4. Aiello LP, Avery RL, Arrigg PG, et al. Vascular endothelial growth factor in ocular fluid of patients with diabetic retinopathy and other retinal disorders. N Engl J Med 1994;331:1480–1487.
5. Hata Y, Nakagawa K, Ishibashi T, Inomata H, Ueno H, Sueishi K. Hypoxia-induced expression of vascular endothelial growth factor by retinal glial cells promotes in vitro angiogenesis. Virchows Arch 1995;426:479–486.
6. Bashshur ZF, Bazarbachi A, Schakal A, Haddad ZA, El Haibi CP, Noureddin BN. Intravitreal bevacizumab for the management of choroidal neovascularization in age-related macular degeneration. Am J Ophthalmol 2006;142:1–9.

7. Gragoudas ES, Adamis AP, Cunningham ET Jr, Feinsod M, Guyer DR. VEGF inhibition study in ocular neovascularization clinical trial group. Pegaptanib for neovascular age-related macular degeneration. N Engl J Med 2004;351:2805–2816.
8. Economopoulou M, Bdeir K, Cines DB, et al. Inhibition of pathologic retinal neovascularization by alpha-defensins. Blood 2005; 106:3831–3838.
9. Konopatskaya O, Churchill AJ, Harper SJ, Bates DO, Gardiner TA. VEGF165b, an endogenous C-terminal splice variant of VEGF, inhibits retinal neovascularization in mice. Mol Vis 2006;12:626–632.
10. Ojima T, Takagi H, Suzuma K, et al. Ephrin A1 inhibits vascular endothelial growth factor-induced intracellular signaling and suppresses retinal neovascularization and blood-retinal barrier breakdown. Am J Pathol 2006;168:331–339.
11. Shen J, Yang X, Xiao WH, Hackett SF, Sato Y, Campochiaro PA. Vasohibin is up-regulated by VEGF in the retina and suppresses VEGF receptor 2 and retinal neovascularization. FASEB J 2006; 20:723–725.
12. Zachary I, Gliki G. Signaling transduction mechanisms mediating biological actions of the vascular endothelial growth factor family. Cardiovasc Res 2001;49:568–581.
13. van Nieuw Amerongen GP, Koolwijk P, Versteilen A, van Hinsbergh VW. Involvement of RhoA/Rho kinase signaling in VEGF-induced endothelial cell migration and angiogenesis in vitro. Arterioscler Thromb Vasc Biol 2003;23:211–217.
14. Nakayama M, Amano M, Katsumi A, et al. Rho-kinase and myosin II activities are required for cell type and environment specific migration. Genes Cells 2005;10:107–117.
15. Ridley AJ, Hall A. The small GTP-binding protein rho regulates the assembly of focal adhesions and actin stress fibers in response to growth factors. Cell 1992;70:389–399.
16. Sun H, Breslin JW, Zhu J, Yuan SY, Wu MH. Rho and ROCK signaling in VEGF-induced microvascular endothelial hyperpermeability. Microcirculation 2006;13:237–247.
17. Zeng L, Xu H, Chew TL, et al. HMG CoA reductase inhibition modulates VEGF-induced endothelial cell hyperpermeability by preventing RhoA activation and myosin regulatory light chain phosphorylation. FASEB J 2005;19:1845–1847.
18. Hoang MV, Whelan MC, Senger DR. Rho activity critically and selectively regulates endothelial cell organization during angiogenesis. Proc Natl Acad Sci U S A 2004;101:1874–1879.
19. Hyvelin JM, Howell K, Nichol A, Costello CM, Preston RJ, McLoughlin P. Inhibition of Rho-kinase attenuates hypoxia-induced angiogenesis in the pulmonary circulation. Circ Res 2005;97:185–191.
20. Ishikura K, Yamada N, Ito M, et al. Beneficial acute effects of rho-kinase inhibitor in patients with pulmonary arterial hypertension. Circ J 2006;70:174–178.
21. Vicari RM, Chaitman B, Keefe D, et al. Efficacy and safety of fasudil in patients with stable angina: a double-blind, placebo-controlled, phase 2 trial. J. Am Coll Cardiol 2005;46:1803–1811.
22. Kishi T, Hirooka Y, Masumoto A, et al. Rho-kinase inhibitor improves increased vascular resistance and impaired vasodilation of the forearm in patients with heart failure. Circulation 2005; 111:2741–2747.
23. Masumoto A, Hirooka Y, Shimokawa H, Hironaga K, Setoguchi S, Takeshita A. Possible involvement of Rho-kinase in the pathogenesis of hypertension in humans. Hypertension 2001;38:1307–1310.
24. Gerber H-P, McMurtrey A, Kowalski J, et al. Vascular endothelial growth factor regulates endothelial cell survival through the phosphatidylinositol 3-kinase/Akt signal transduction pathway. J Biol Chem 1998;273:30336–30343.
25. Dimmeler S, Dernbach E, Zeiher AM. Phosphorylation of the endothelial nitric oxide synthase at ser-1177 is required for VEGF-induced endothelial cell migration. FEBS Lett 2000;477:258–262.
26. Nakao S, Kuwano T, Tsutsumi-Miyahara C, et al. Infiltration of COX-2-expressing macrophages is a prerequisite for IL-1 beta-induced neovascularization and tumor growth. J Clin Invest 2005;115:2979–2991.
27. Noda Y, Hata Y, Hisatomi T, et al. Functional properties of hyalocytes under PDGF-rich conditions. Invest Ophthalmol Vis Sci 2004;45:2107–2114.
28. Cascone I, Giraudo E, Caccavari F, et al. Temporal and spatial modulation of Rho GTPases during in vitro formation of capillary vascular network. Adherens junctions and myosin light chain as targets of Rac1 and RhoA. J Biol Chem 2003;278:50702–50713.
29. Eliceiri BP, Klemke R, Stromblad S, Cheresh DA. Integrin alphavbeta3 requirement for sustained mitogen-activated protein kinase activity during angiogenesis. J Cell Biol 1998;140:1255–1263.
30. Mavria G, Vercoulen Y, Yeo M, et al. ERK–MAPK signaling opposes Rho-kinase to promote endothelial cell survival and sprouting during angiogenesis. Cancer Cell 2006;9:33–44.
31. Gliki G, Wheeler-Jones C, Zachary I. Vascular endothelial growth factor induces protein kinase C (PKC)-dependent Akt/PKB activation and phosphatidylinositol 3'-kinase-mediates PKC delta phosphorylation: role of PKC in angiogenesis. Cell Biol Int 2002;26:751–759.
32. Shimokawa H, Seto M, Katsumata N, et al. Rho-kinase-mediated pathway induces enhanced myosin light chain phosphorylations in a swine model of coronary artery spasm. Cardiovasc Res 1999;43: 1029–1039.
33. Wolfrum S, Dendorfer A, Rikitake Y, et al. Inhibition of Rho-kinase leads to rapid activation of phosphatidylinositol 3-kinase/protein kinase Akt and cardiovascular protection. Arterioscler Thromb Vasc Biol 2004;24:1842–1847.
34. Hirayama K, Hata Y, Noda Y, et al. The involvement of the rho-kinase pathway and its regulation in cytokine-induced collagen gel contraction by hyalocytes. Invest Ophthalmol Vis Sci 2004;45: 3896–3903.
35. Miura M, Hata Y, Hirayama K, et al. Critical role of the Rho-kinase pathway in TGF-beta2-dependent collagen gel contraction by retinal pigment epithelial cells. Exp Eye Res 2006;82:849–859.

*The American Journal of Pathology, Vol. 173, No. 5, November 2008*

*DOI: 10.2353/ajpath.2008.080466*

*Cell Injury, Repair, Aging and Apoptosis*

# Inhibition of Nuclear Translocation of Apoptosis-Inducing Factor Is an Essential Mechanism of the Neuroprotective Activity of Pigment Epithelium-Derived Factor in a Rat Model of Retinal Degeneration

Yusuke Murakami,*† Yasuhiro Ikeda,† Yoshikazu Yonemitsu,‡ Mitsuho Onimaru,* Kazunori Nakagawa,* Ri-ichiro Kohno,† Masanori Miyazaki,† Toshio Hisatomi,† Makoto Nakamura,§ Takeshi Yabe,¶ Mamoru Hasegawa,‖ Tatsuro Ishibashi,† and Katsuo Sueishi*

*From the Department of Pathology,* Division of Pathophysiological and Experimental Pathology, and the Department of Ophthalmology,† Graduate School of Medical Sciences, Kyushu University, Fukuoka; the Department of Gene Therapy,‡ Chiba University Graduate School of Medicine, Chiba; the Department of Organs Therapeutics,§ Division of Ophthalmology, Kobe University Graduate School of Medicine, Kobe; the Kitasato Institute for Life Sciences,¶ Kitasato University, Tokyo; and DNAVEC Corporation,‖ Ibaraki, Japan*

**Photoreceptor apoptosis is a critical process of retinal degeneration in retinitis pigmentosa (RP), a group of retinal degenerative diseases that result from rod and cone photoreceptor cell death and represent a major cause of adult blindness. We previously demonstrated the efficient prevention of photoreceptor apoptosis by intraocular gene transfer of pigment epithelium-derived factor (PEDF) in animal models of RP; however, the underlying mechanism of the neuroprotective activity of PEDF remains elusive. In this study, we show that an apoptosis-inducing factor (AIF)-related pathway is an essential target of PEDF-mediated neuroprotection. PEDF rescued serum starvation-induced apoptosis, which is mediated by AIF but not by caspases, of R28 cells derived from the rat retina by preventing translocation of AIF into the nucleus. Nuclear translocation of AIF was also observed in the apoptotic photoreceptors of Royal College of Surgeons rats, a well-known animal model of RP that carries a mutation of the *Mertk* gene. Lentivirus-mediated retinal gene transfer of PEDF prevented the nuclear translocation of AIF *in vivo*, resulting in the inhibition of the apoptotic loss of their photoreceptors in association with up-regulated Bcl-2 expression, which mediates the mitochondrial release of AIF. These findings clearly demonstrate that AIF is an essential executioner of photoreceptor apoptosis in inherited retinal degeneration and provide a therapeutic rationale for PEDF-mediated neuroprotective gene therapy for individuals with RP.** ***(Am J Pathol 2008, 173:1326–1338; DOI: 10.2353/ajpath.2008.080466)***

Retinitis pigmentosa (RP) is a group of retinal degenerative diseases resulting from rod and cone photoreceptor cell death, and a major cause of blindness in adults. RP is caused by mutation in various genes expressed in photoreceptors, the retinal pigment epithelium (RPE) and choriocapillaris of the eye[1,2]; on the other hand, photoreceptors undergo a common mode of cell death, apoptosis.[3,4] Despite extensive efforts to better understand and treat RP, the mechanisms underlying the photoreceptor apoptosis are still unclear and these diseases remain intractable.

Supported in part by the Japanese Ministry of Education, Culture, Sports, Science, and Technology (grants-in-aid 16390118, 17689047, and 19209012 to Y.I., Y.Y., and K.S.).

Accepted for publication August 7, 2008.

Competing Interest Statement: Y.Y. is a member of the Scientific Advisory Board of DNAVEC Corporation.

Supplemental material for this article can be found on *http://ajp.amjpathol.org*.

Address reprint requests to Katsuo Sueishi, M.D., Ph.D., Division of Pathophysiological and Experimental Pathology, Department of Pathology, Graduate School of Medical Sciences, Kyushu University, 3-1-1 Maidashi, Higashi-ku, Fukuoka, 812-8582, Japan. E-mail: sueishi@pathol1.med.kyushu-u.ac.jp.

Pigment epithelium-derived factor (PEDF) is a 50-kDa secreted glycoprotein that was isolated from the conditioned medium of human RPE,[5,6] and shows both neuroprotective and anti-angiogenic properties.[7,8] Vitreous samples from patients with RP contain significantly lower levels of PEDF than those from patients with other retinal conditions.[9] We previously demonstrated that a lentiviral vector based on the simian immunodeficiency virus from African green monkeys (SIVagm) showed sustained transgene expression in RPE of the rat retina,[10] and SIV-mediated retinal gene transfer of PEDF efficiently prevented photoreceptor apoptosis in Royal College of Surgeons (RCS) rats, an animal model of retinal degeneration caused by a *Mertk* mutation.[11] In addition, these protective effects of PEDF have also been observed in rds mice (M. Miyazaki et al, unpublished observations) and rd1 mice,[12] in which the deficits of photoreceptors are caused by different mutations, suggesting the possibility that PEDF might suppress a common pathway leading to the photoreceptor apoptosis. Several studies have demonstrated the direct protective effects on neuronal cells in culture,[13] but the precise mechanism by which PEDF acts on photoreceptors remains unknown.

The caspase family has emerged as a central regulator of apoptosis, especially in the developmental stages. However, recent evidence indicates that apoptosis can be induced by a caspase-independent pathway in several pathological states.[14] Apoptosis-inducing factor (AIF), a flavoprotein in the mitochondrial intermembrane space, has been identified as a caspase-independent apoptotic inducer,[15,16] and plays a prosurvival role through its redox activity under normal conditions.[17,18] AIF translocates to the nucleus during the apoptotic process, and causes peripheral chromatin condensation and large-scale fragmentation of DNA.[19,20] The translocation of AIF has been implicated in several types of neuronal demise, including photoreceptor apoptosis, and has been shown to contribute significantly to the apoptotic process.[21–23]

In the present study, we investigated the signaling pathways related to photoreceptor apoptosis that could be targets of the neuroprotective activity of PEDF *in vitro* and *in vivo*. We found that the nuclear translocation of AIF occurs in apoptotic photoreceptors in RCS rats, and that PEDF targets this process, resulting in the prevention of the apoptosis.

## Materials and Methods

### Reagents and SIV Vectors

The recombinant human (rhPEDF) was prepared as previously described.[24] His-tagged rhPEDF cloned into pCEP4 vector was isolated from medium conditioned by HEK293 cells. Polyclonal anti-hPEDF antibody was purchased from R&D Systems (Minneapolis, MN). The broad range caspase inhibitor Z-VAD-fmk was obtained from Peptide Institute (Osaka, Japan). Staurosporine was from Alomone Labs (Jerusalem, Israel). To produce third-generation recombinant SIVagm-based lentiviral vectors, HEK293T cells were transfected with the packaging vector, the gene transfer vectors encoding hPEDF (SIV-hPEDF) driven by the cytomegalovirus promoter, the Rev expression vector, and the envelope vector, pVSV-G (Clontech Laboratories, Inc., Mountain View, CA). The SIV vector lacking a transgene cassette (SIV-Empty) was used as the control vector. A U3 region in the 3′ and 5′ long terminal repeat of the SIVagm was deleted to induce self-inactivation. The virus titer was determined by a transduction of the HEK293T cells as expressed in transducing Us/ml, and these viruses were kept at −80°C until just before use.

### Cell Culture and Viability Assay

R28 cells, an immortalized retinal precursor cell line derived from the rat retina at postnatal day 6, were the kind gift of Gail M. Seigel (The State University of New York, Buffalo, NY). R28 cells were cultured in Dulbecco's modified Eagle's medium-high glucose with 10% fetal bovine serum, 1× minimum essential medium, 1 × 10 mmol/L nonessential amino acids, 0.37% sodium bicarbonate, and 10 mg/ml gentamicin (Invitrogen, Carlsbad, CA). To induce cell death by serum starvation, R28 cells at 50% confluence were washed with phosphate-buffered saline (PBS) twice, and the culture medium was replaced with 100 μl of serum-free medium. After 6 hours for synchronization, rhPEDF or PBS was added to each well at the indicated concentration. After incubation for 48 hours, the cell viability was assessed by a Cell Counting Kit-8 (Dojindo Laboratories, Kumamoto, Japan). This assay is based on the cleavage of 2-(2-methoxy-4-nitrophenyl)-3-(4-nitrophenyl)-5-(2,4-disulfophenyl)-2H-tetrazolium, monosodium salt (WST-8) to formazan dye by the mitochondrial dehydrogenase enzyme. After incubation with WST-8 for 2 hours at 37°C, the absorbance was measured at 450 nm using a microplate leader. The absorbance was directly proportional to the number of living cells (data not shown).

### Animals

Adult RCS rats and age-matched Wistar rats were maintained humanely with proper institutional approval, and in accordance with the statement of the Association for Research in Vision and Ophthalmology. All animal experiments were performed under approved protocols and in accordance with the recommendations for the proper care and use of laboratory animals by the Committee for Animals, Recombinant DNA, and Infectious Pathogens Experiments at Kyushu University and according to The Law (no.105) and Notification (no.6) of the Japanese Government.

### Gene Transfer Procedures

The subretinal injection of each solution was performed as previously described.[11,25] Briefly, 3-week-old RCS rats were anesthetized by inhalation ether. A 30-gauge needle was inserted into the subretinal space of the peripheral retina in the nasal hemisphere via an external

transscleral transchoroidal approach. The vector solution (SIV-hPEDF or SIV-Empty; $2.5 \times 10^7$ transducing U/ml × 10 μl) was injected, and excess solution from the injection site was washed out using PBS. Approximately 3 μl of solution remained in the subretinal space (data not shown). The appearance of a dome-shaped retinal detachment confirmed the subretinal delivery. Eyes that sustained prominent surgical trauma, such as retinal or subretinal hemorrhage or bacterial infection, were excluded from this examination.

### *Histological Examination*

At 2 weeks after gene transfer, the eyes of animals were enucleated and frozen in liquid nitrogen, and 5-μm-thick cryosections were prepared along the horizontal meridian. The sections were stained with hematoxylin and eosin, and the number of photoreceptors was counted per 100 μm at 10 points as previously described (A1 to A5: from the ora serrata to the optic nerve of the nasal hemisphere; A6 to A10: from the optic nerve to the ora serrata of the temporal hemisphere).[11]

### *Immunocytochemistry*

R28 cells were fixed in 4% paraformaldehyde for 15 minutes, and then rinsed with PBS at room temperature. The cells were blocked with 3% nonfat dried milk and labeled with rabbit anti-AIF antibody (1:100; Cell Signaling Technology, Danvers, MA) at 4°C for 24 hours. After biotinylated goat anti-rabbit IgG (H+L) (1:200; Vector Laboratories, Burlingame, CA) was used as a secondary antibody, the cells were incubated with r-phycoerythrin (PE)-conjugated or fluorescein isothiocyanate-conjugated streptavidin (1:100; BD Biosciences, San Diego, CA). After labeling, propidium iodide or 4,6-diamidino-2-phenylindole (DAPI) was used to counterstain the nuclei. Immunofluorescence images were acquired using an Olympus BX51 microscope with a fluorescent attachment (Tokyo, Japan). For negative controls, the primary antibody was omitted.

### *Immunohistochemistry*

Rats were sacrificed under deep anesthesia. The eyes were removed and frozen in OCT compound (Sakura Finetechnical Co., Tokyo, Japan). Five-μm-thick sections were cut, air-dried, and fixed in cold acetone for 10 minutes. For a primary antibody, rabbit anti-AIF antibody (1:100; Cell Signaling Technology) was used. The specimens were imaged with a laser-scanning confocal microscope (LSM-GB200, Olympus).

### *Terminal dUTP Nick-End Labeling (TUNEL) Staining*

The TUNEL procedure and quantification of TUNEL-positive cells were performed using an ApopTag fluorescein direct *in situ* apoptosis detection kit (Chemicon International, Temecula, CA) for R28 cultures or an Apoptosis Detection TACS TdT Kit (R&D Systems) for retinal sections according to the instructions of the manufacturer. The number of TUNEL-positive cells was counted in a masked manner.

### *Flow Cytometry Analysis*

The population of early apoptotic cells was analyzed using an Annexin V-PE Apoptosis Detection Kit I (BD Biosciences). After serum starvation, R28 cells were harvested, washed twice with ice-cold PBS, and resuspended in 100 μl of calcium-binding buffer (10 mmol/L Hepes/NaOH, pH 7.4, 140 mmol/L NaCl, 2.5 mmol/L $CaCl_2$). The cells were double-labeled with Annexin V-PE (1:20) for the assessment of phosphatidylserine exposure and 7-amino-actinomycin D (7-AAD) (1:20) for cell viability analysis. After 15 minutes of incubation in the dark, the cells were diluted with 400 μl of binding buffer. Samples were analyzed in a FACScan flow cytometer (Becton Dickinson, San Jose, CA) using the program CellQuest (Becton Dickinson) for subsequent data treatment. A total of 5000 events per sample were acquired, and Annexin V-PE-positive and 7-AAD-negative events were defined as early apoptotic cells.

### *Western Blotting*

Eighty μg of protein was separated on sodium dodecyl sulfate-polyacrylamide gel electrophoresis and transferred to the membrane. After blocking with 3% nonfat dried milk, the membrane was reacted with anti-AIF antibody (Calbiochem, San Diego, CA), anti-cleaved caspase-3, anti-Bcl-2, or anti-Bax antibody (Cell Signaling Technology). The immunoreactivity was visualized using the ECL Plus detection reagents (Amersham Biosciences, Buckinghamshire, UK).

### *Enzyme-Linked Immunosorbent Assay (ELISA)*

The protein contents in rat eyes were determined using an ELISA kit for human PEDF (not available for rat PEDF; Chemicon International). For ocular tissue preparation, conjunctival and muscular tissues were removed from enucleated eyes. The eyes were washed with PBS, minced with scissors in 500 μl of 1× lysis buffer with a protease inhibitor cocktail, and centrifuged at 15,000 rpm for 5 minutes at 4°C. The supernatants were subjected to ELISA according to the manufacturer's instructions.

### *RNAi*

AIF siRNA was synthesized with the sequence 5'-GCAACCUAGUAUACUUCUUTT-3'. The scrambled counterpart, control siRNA, had the sequence 5'-GCAUCGAAUAUUCUAC-CUUTT-3'. The sequence of Bcl-2 siRNA was 5'-AUGGAUGUACUUCAUCACGAUCUCC-3', and the negative control kit Medium GC was used as a control (Invitrogen). Transfection of 40 nmol/L siRNA was performed using Lipofectamine 2000 reagent (Invitrogen) according to the manufacturer's instructions.

### *RNA Extraction and Quantitative Real-Time Polymerase Chain Reaction (PCR)*

The procedures for RNA extraction were described previously.[26] The total RNA was extracted from the R28 cells or the neural retina by Isogen (Nippon Gene Co., Osaka, Japan) followed by treatment with RNase-free DNase I. The RNA was then reverse-transcribed and amplified with the TaqMan EZ RT-PCR kit and a sequence detection system, model 7000 (Applied Biosystems, Foster City, CA). The PCR primers used in this study were as follows: rat Bcl-2 forward, 5′-CTGGGATGCCTTTGTGGAA-3′; rat Bcl-2 reverse, 5′-CAGAGACAGCCAGGAGAAATCA-3′; rat Bcl-2 hybridization probe, 5′-FAM-ATGGCCCCAGCATGCGACCTC-TAMRA-3′; rat Bax forward, 5′-CGTGGTTGCCCTCT TCTACTTT-3′, rat Bax reverse, 5′-TGATCAGCTCGGGCACTTTA-3′; rat Bax hybridization probe, 5′-FAM-CTAGCAAACTGGTGCTCAAGGCCCTG-TAMRA-3′; rat β-actin forward, 5′-CCCTGGCTCCTAGCACCAT-3′; rat β-actin reverse, 5′-CCTGCTTGC-TGATCCACATCT-3′; and rat β-actin hybridization probe, 5′-FAM-CCTGGCCTCACTGTCCACCTTCCA-TAMRA-3′. The expression level of the target gene was normalized by the β-actin level in each sample.

### *MitoTracker Staining*

R28 cells were incubated with a 50 nmol/L solution of MitoTracker Orange CMTMRos (Invitrogen), a derivative of tetramethylrosamine, for 15 minutes at 37°C. The MitoTracker probe passively diffuses across the plasma membrane and accumulates in active mitochondria, driven by the mitochondrial inner transmembrane potential.[27,28] After incubation, the cells were fixed in 4% paraformaldehyde for 15 minutes, labeled with DAPI, and observed under a fluorescence microscope.

### *Statistical Analyses*

All values were expressed as the mean ± SD. The data were analyzed by the two-tailed unpaired Student's *t*-test. Numbers per group were as indicated. A *P* value less than 0.05 was considered statistically significant.

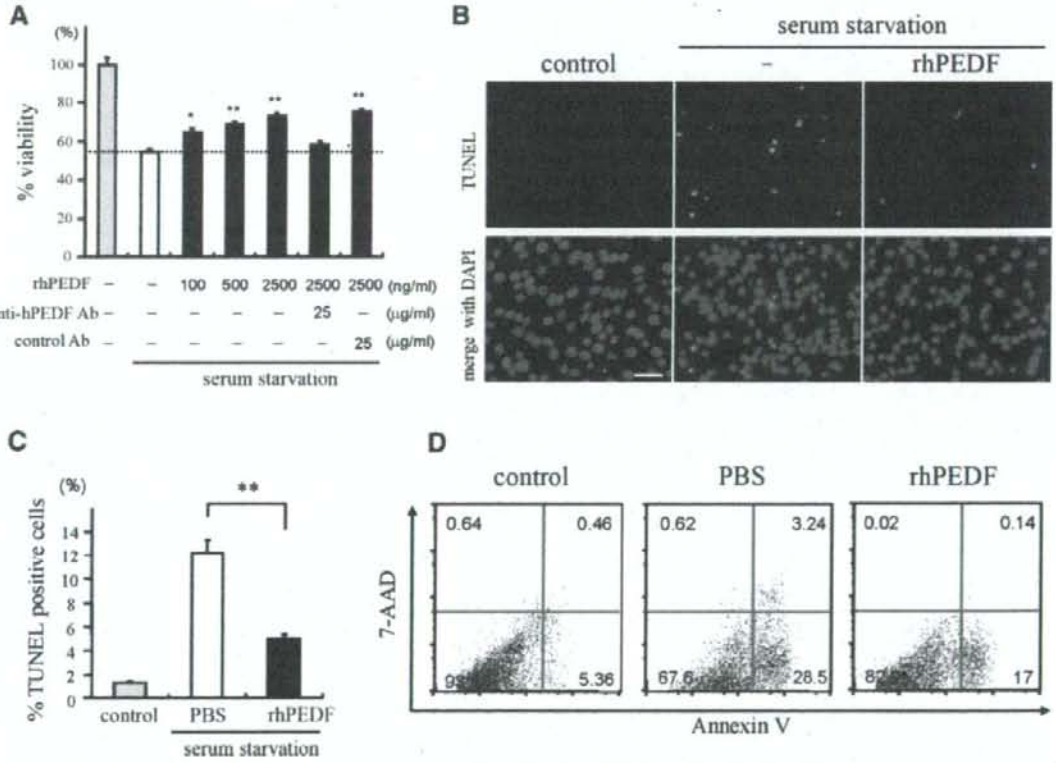


**Figure 1.** PEDF rescues apoptosis induced by serum starvation in R28 cells. **A:** The effect of PEDF on cell viability. R28 cells were serum-deprived and treated with PBS or rhPEDF at the indicated doses. After 48 hours of culturing, the cell viability was assessed by WST-8 colorimetric assay ($n = 4$ each). The effect of PEDF was reversed by anti-PEDF antibody but not by nonimmune control antibody. $^{*}P < 0.05$ and $^{**}P < 0.01$ versus PBS-treated samples. **B** and **C:** TUNEL staining (**B**) and quantitative analysis of the TUNEL-positive apoptotic nuclei (**C**) in serum-starved R28 cells treated with PBS (white bar) or rhPEDF (black bar) ($n = 5$ each). The cells growing in serum-containing medium were used as controls (gray bar). $^{**}P < 0.01$. **D:** Flow cytometry analysis of the apoptotic population after 48 hours of serum starvation. Cells were stained with Annexin V and 7-AAD. The percentages of Annexin V-positive and 7-AAD-negative early apoptotic cells were 28.3 ± 0.15% in PBS-treated cells and 17.7 ± 0.34% in rhPEDF-treated cells ($n = 4$ each). Scale bar = 50 μm.